Contents

List of Figures

1. Microscopic dielectric theory

In this chapter we revisit the classical dielectric response of a material and outline it's connection to a quantum mechanical expectation value of the so-called density-fluctuation operator. The evaluation of this expectation value is the main goal of the Bethe-Salpeter equation formalism discussed in section 2.3.4 and chapter 3.

In section 1.1 we first recapitulate Maxwell's equations within a medium and discuss the so-called material equations. The material equations constitute linear response functions which link external and induced quantities of Maxwell's theory. The microscopic dielectric tensor ε is introduced in section 1.2 as the main material equation of interest, and the longitudinal and transversal response formalism is discussed. In section 1.3 we then demonstrate how ε can be computed quantum mechanically using first-order time-dependent perturbation theory. In section 1.4 the connection to the dynamical structure factor and to the optical absorption spectrum is given. Lastly, in section 1.5 the case of a crystalline system is discussed. In this chapter we mainly follow the notation of [1] and keep the notation in SI-units.

1.1. Microscopic Maxwell equations

When considering the interaction of a solid with an external electromagnetic field, the Maxwell equations are commonly written in terms of external and induced quantities. For example, the total charge density in the material can be split into the charge density of the unperturbed system ρ^0, an externally introduced charge density ρ^{ext}, and an induced charge density ρ^{ind} that describes the change of ρ^0 due to ρ^{ext}:

$$\rho^{\text{total}} = \rho^{\text{ext}} + \rho^{\text{ind}} + \rho^0. \tag{1.1}$$

By doing the same for the current and the fields, the Maxwell equations can be solved excluding the unperturbed quantities. Then,

$$\rho = \rho^{\text{ext}} + \rho^{\text{ind}} \tag{1.2}$$

denotes the charge density difference with respect to the unperturbed system. In the following we use the same notation for the current and fields. The induced charge density ρ^{ind} and the induced current $\boldsymbol{j}^{\text{ind}}$ are usually described in terms of the *polarization field* $\boldsymbol{P}$ and the *magnetization field* $\boldsymbol{M}$, according to

$$\rho^{\text{ind}} = \nabla \cdot \boldsymbol{P} \quad \text{and} \quad \boldsymbol{j}^{\text{ind}} = \frac{\partial \boldsymbol{P}}{\partial t} + \nabla \times \boldsymbol{M}. \tag{1.3}$$

The fields $\boldsymbol{P}$ and $\boldsymbol{M}$ are not uniquely defined, since $\tilde{\boldsymbol{P}} = \boldsymbol{P} - \nabla \times L$ and $\tilde{\boldsymbol{M}} = \boldsymbol{M} + \frac{\partial L}{\partial t}$ yield the same density and current for any function L. By setting $\boldsymbol{M} = \frac{1}{\mu_0}\boldsymbol{B}^{\mathrm{ind}}$ and $\boldsymbol{P} = -\varepsilon_0 \boldsymbol{E}^{\mathrm{ind}}$ Maxwell's equations neatly separate into induced and external fields:

$$\begin{aligned} \nabla \cdot \boldsymbol{B} &= 0 & \nabla \times \boldsymbol{E} + \partial_t \boldsymbol{B} &= 0 && (1.4a)\\ \nabla \times \boldsymbol{B}^{\mathrm{ext}} - c_0^{-2}\partial_t \boldsymbol{E}^{\mathrm{ext}} &= \mu_0 \boldsymbol{j}^{\mathrm{ext}} & \nabla \cdot \boldsymbol{E}^{\mathrm{ext}} &= \varepsilon_0^{-1}\rho^{\mathrm{ext}} && (1.4b)\\ \nabla \times \boldsymbol{B}^{\mathrm{ind}} - c_0^{-2}\partial_t \boldsymbol{E}^{\mathrm{ind}} &= \mu_0 \boldsymbol{j}^{\mathrm{ind}} & \nabla \cdot \boldsymbol{E}^{\mathrm{ind}} &= -\varepsilon_0^{-1}\rho^{\mathrm{ind}}. && (1.4c) \end{aligned}$$

The fields can also be expressed in terms of the electrostatic scalar potential φ and the magnetic vector potential $\boldsymbol{A}$ as

$$\boldsymbol{E}(\boldsymbol{r},t) = -\nabla \cdot \varphi(\boldsymbol{r},t) - \partial_t \boldsymbol{A}(\boldsymbol{r},t) \quad \text{and} \quad \boldsymbol{B}(\boldsymbol{r},t) = \nabla \times \boldsymbol{A}(\boldsymbol{r},t). \tag{1.5}$$

Additionally to the set of equations (1.4), a *material equation* is needed to connect the induced quantities to the external ones. For a sufficiently small perturbation they are given by *linear response functions* of the form

$$F_\alpha^{\mathrm{ind}}(\boldsymbol{r},t) = \sum_\beta \iint R^{\alpha\beta}(\boldsymbol{r},\boldsymbol{r}',t-t')F_\beta^{\mathrm{ext}}(\boldsymbol{r}',t')\,\mathrm{d}^3r'\,\mathrm{d}t', \quad \text{symbolically} \quad \boldsymbol{F}^{\mathrm{ind}} = R\boldsymbol{F}^{\mathrm{ext}}, \tag{1.6}$$

where R is non-zero only for $t > t'$ to ensure causality [2]. One example of such a response function is the electrical *susceptibility* χ that relates the induced current to the external electric field

$$\partial_t \boldsymbol{j}^{\mathrm{ind}} = \chi \boldsymbol{E}^{\mathrm{ext}}. \tag{1.7}$$

1.2. Microscopic dielectric tensor

The concept of the response functions can be generalized to also include relations between the total fields to the external ones. In particular, we are interested in the *microscopic dielectric tensor* ε^{ij} that relates the external electric field $\boldsymbol{E}^{\mathrm{ext}}$ to the total perturbing electric field $\boldsymbol{E}$. It is the key quantity in describing the response of a system to incoming light or penetrating electrons and it is defined as

$$E_i^{\mathrm{ext}}(\boldsymbol{r},t) = \iint \sum_j \varepsilon^{ij}(\boldsymbol{r},\boldsymbol{r}',t-t')E_j(\boldsymbol{r}',t')\,\mathrm{d}^3r\,\mathrm{d}t', \quad \text{symbolically} \quad \boldsymbol{E}^{\mathrm{ext}} = \varepsilon\boldsymbol{E}. \tag{1.8}$$

Decomposing the electric fields into a curl-free (longitudinal) E_{L} and a divergence-free (transversal) E_{T} component

$$\boldsymbol{E} = \boldsymbol{E}_{\mathrm{L}} + \boldsymbol{E}_{\mathrm{T}} \quad \text{where} \quad \nabla \cdot \boldsymbol{E}_{\mathrm{T}} = \nabla \times \boldsymbol{E}_{\mathrm{L}} = 0, \tag{1.9}$$

eq. (1.8) can be split into longitudinal (L) and transversal (T) subspaces as

$$\begin{pmatrix} \boldsymbol{E}_{\mathrm{L}}^{\mathrm{ext}} \\ \boldsymbol{E}_{\mathrm{T}}^{\mathrm{ext}} \end{pmatrix} = \begin{pmatrix} \varepsilon_{\mathrm{LL}} & \varepsilon_{\mathrm{LT}} \\ \varepsilon_{\mathrm{TL}} & \varepsilon_{\mathrm{TT}} \end{pmatrix} \begin{pmatrix} \boldsymbol{E}_{\mathrm{L}} \\ \boldsymbol{E}_{\mathrm{T}} \end{pmatrix}. \tag{1.10}$$

In the following, we assume that the external perturbation is purely longitudinal and that the resulting induced current is also purely longitudinal. Then, only the longitudinal-longitudinal response is needed to describe the dielectric properties of the system:

$$\boldsymbol{E}^{\mathrm{ext}} = \boldsymbol{E}_{\mathrm{L}}^{\mathrm{ext}} \approx \varepsilon_{\mathrm{LL}} \boldsymbol{E}_{\mathrm{L}}. \tag{1.11}$$

Using the Coulomb-gauge ($\nabla \cdot \boldsymbol{A} = 0$), this can be equivalently formulated in terms of the *longitudinal microscopic dielectric function* that relates the external and the total perturbing scalar potential

$$\varphi_{\mathrm{ext}}(\boldsymbol{r}, t) = \iint \varepsilon(\boldsymbol{r}, \boldsymbol{r}', t - t')\varphi(\boldsymbol{r}', t')\,\mathrm{d}^3 r'\,\mathrm{d}t'\,. \tag{1.12}$$

Under these conditions the Fourier coefficients of the tensor $\varepsilon_{\mathrm{LL}}$ and the function ε are related by

$$\varepsilon_{\mathrm{LL}}^{\alpha\beta}(\boldsymbol{q}, \boldsymbol{q}', \omega) = \frac{q_\alpha \varepsilon(\boldsymbol{q}, \boldsymbol{q}', \omega) q'_\beta}{|\boldsymbol{q}'|^2}. \tag{1.13}$$

In analogy to eq. (1.12) one can introduce the *(longitudinal) susceptibility* χ

$$\rho_{\mathrm{ind}}(\boldsymbol{r}, t) = \iint e^2 \chi(\boldsymbol{r}, \boldsymbol{r}', t - t')\varphi_{\mathrm{ext}}(\boldsymbol{r}', t')\,\mathrm{d}^3 r'\,\mathrm{d}t' \tag{1.14}$$

and the *(longitudinal) polarizability* P

$$\rho_{\mathrm{ind}}(\boldsymbol{r}, t) = \iint e^2 P(\boldsymbol{r}, \boldsymbol{r}', t - t')\varphi(\boldsymbol{r}', t')\,\mathrm{d}^3 r'\,\mathrm{d}t'\,. \tag{1.15}$$

The dielectric function and its inverse can be expressed in terms of χ and P as

$$\varepsilon^{-1} = 1 + v\chi \quad \text{and} \quad \varepsilon = 1 - vP, \tag{1.16}$$

where v denotes the Coulomb potential. The response functions P and χ are in turn related to each other by the Dyson equation

$$\chi = P + Pv\chi. \tag{1.17}$$

Remark. The approximation of a purely longitudinal external electric field made in eq. (1.11) is reasonable for the description of the response to an electron passing through the system. The electric field of light, on the other hand, is purely transversal and would require a response function relating the external and total vector potential $\boldsymbol{A}$ (in the Coulomb gauge). Fortunately, in the limit of long wave-lengths or vanishing $\boldsymbol{q}$, it was shown that the purely longitudinal and purely transversal response become equal in crystalline systems of cubic [3] and lower [4] symmetry.

1.3. Susceptibility from time-dependent perturbation theory

The variation of an observable $f(t)$ due to a perturbation $\hat{\mathrm{H}}'(t)$, which was switched on at time t_0, can be computed by first-order time-dependent perturbation theory according to [5]

$$\tilde{f}(t) = \langle \Psi_\mathrm{S}(t) | \hat{\mathrm{f}}_\mathrm{S}(t) | \Psi_\mathrm{S}(t) \rangle - \left\langle \Psi^0_\mathrm{H} \middle| \hat{\mathrm{f}}_\mathrm{H}(t) \middle| \Psi^0_\mathrm{H} \right\rangle = \frac{\mathrm{i}}{\hbar} \int_{t_0}^{t} \left\langle \Psi^0_\mathrm{H} \middle| \left[\hat{\mathrm{H}}'_\mathrm{H}(t'), \hat{\mathrm{f}}_\mathrm{H}(\boldsymbol{r}, t) \right]_- \middle| \Psi^0_\mathrm{H} \right\rangle \mathrm{d}t' \,, \tag{1.18}$$

where the subscript H (S) denotes the Heisenberg (Schrödinger) picture and Ψ^0_H is the normalized ground state of the unperturbed system, while $\Psi_\mathrm{S}(t)$ is the exact state of the perturbed system which evolves from $\Psi^0_\mathrm{S}(t_0)$. If we consider a perturbation due to an external scalar potential, $\hat{\mathrm{H}}'$ takes on the form

$$\hat{\mathrm{H}}'_\mathrm{H}(t) = \int \hat{\rho}_\mathrm{H}(\boldsymbol{r}, t) \varphi^\mathrm{ext}(\boldsymbol{r}, t) \, \mathrm{d}^3 r = \int \hat{\mathrm{n}}_\mathrm{H}(\boldsymbol{r}, t) e \varphi^\mathrm{ext}(\boldsymbol{r}, t) \, \mathrm{d}^3 \boldsymbol{r} \,, \tag{1.19}$$

and the variation of the density $n(\boldsymbol{r})$ follows as

$$\tilde{n}(\boldsymbol{r}, t) = \frac{\mathrm{i}}{\hbar} \int_{t_0}^{t} \mathrm{d}t' \int \mathrm{d}^3 r' \, e \varphi^\mathrm{ext}(\boldsymbol{r}', t') \left\langle \Psi^0_\mathrm{H} \middle| \left[\hat{\mathrm{n}}_\mathrm{H}(\boldsymbol{r}', t'), \hat{\mathrm{n}}_\mathrm{H}(\boldsymbol{r}, t) \right]_- \middle| \Psi^0_\mathrm{H} \right\rangle . \tag{1.20}$$

This can be rewritten in terms of the *density deviation operator* $\hat{\hat{\mathrm{n}}}_H$

$$\hat{\hat{\mathrm{n}}}_\mathrm{H} = \hat{\mathrm{n}}_\mathrm{H} - \left\langle \Psi^0_\mathrm{H} \middle| \hat{\mathrm{n}}_\mathrm{H} \middle| \Psi^0_\mathrm{H} \right\rangle \tag{1.21}$$

by simply replacing $\hat{\mathrm{n}}_\mathrm{H}$ with $\hat{\hat{\mathrm{n}}}_\mathrm{H}$ in eq. (1.20). Then, the susceptibility defined in eq. (1.14) can be identified with the *retarded density correlation function*

$$\begin{aligned} \chi^\mathrm{R}(\boldsymbol{r}, \boldsymbol{r}', t - t') = \frac{\delta n_\mathrm{ind}(\boldsymbol{r}, t)}{\delta e \varphi_\mathrm{ext}(\boldsymbol{r}', t')} &= \frac{-i}{\hbar} \theta(t - t') \left\langle \Psi^0_\mathrm{H} \middle| \left[\hat{\hat{\mathrm{n}}}_\mathrm{H}(\boldsymbol{r}, t), \hat{\hat{\mathrm{n}}}_\mathrm{H}(\boldsymbol{r}', t') \right]_- \middle| \Psi^0_\mathrm{H} \right\rangle \\ &= \frac{-i}{\hbar} \theta(t - t') \left\langle \Psi^0_\mathrm{H} \middle| \left[\hat{\hat{\mathrm{n}}}_\mathrm{H}(\boldsymbol{r}, t - t' + t_0), \hat{\hat{\mathrm{n}}}_\mathrm{H}(\boldsymbol{r}', t_0) \right]_- \middle| \Psi^0_\mathrm{H} \right\rangle . \end{aligned} \tag{1.22}$$

Since $\hat{\mathrm{H}}$ is time-independent, it only depends on the time difference $t - t'$. Equation (1.22) thus connects the classical dielectric response to a quantum mechanical expectation value in the unperturbed system. In order to apply many-body perturbation methods, it is necessary to introduce the related *time-ordered density correlation function*

$$\begin{aligned} \chi^\mathrm{T}(\boldsymbol{r}, \boldsymbol{r}', t - t') &= \frac{-i}{\hbar} \left\langle \Psi^0_\mathrm{H} \middle| \hat{\mathcal{T}} \left[\hat{\hat{\mathrm{n}}}_\mathrm{H}(\boldsymbol{r}, t) \hat{\hat{\mathrm{n}}}_\mathrm{H}(\boldsymbol{r}', t') \right] \middle| \Psi^0_\mathrm{H} \right\rangle \\ &= \frac{-i}{\hbar} \left\langle \Psi^0_\mathrm{H} \middle| \hat{\mathcal{T}} \left[\hat{\hat{\mathrm{n}}}_\mathrm{H}(\boldsymbol{r}, t - t' + t_0) \hat{\hat{\mathrm{n}}}_\mathrm{H}(\boldsymbol{r}', t_0) \right] \middle| \Psi^0_\mathrm{H} \right\rangle , \end{aligned} \tag{1.23}$$

where $\hat{\mathcal{T}}$ is the Wick's time-ordering operator. There is a straightforward relation between the retarded and time-ordered correlation functions [5]:

$$\chi^\mathrm{T}(\boldsymbol{r}, \boldsymbol{r}', \omega) = \chi^\mathrm{R}(\boldsymbol{r}, \boldsymbol{r}', \omega) \quad \text{and} \quad \chi^\mathrm{R}(\boldsymbol{r}, \boldsymbol{r}', -\omega) = \left(\chi^\mathrm{R}(\boldsymbol{r}, \boldsymbol{r}', \omega) \right)^* , \omega > 0. \tag{1.24}$$

The methods needed to evaluate eqs. (1.22) and (1.23) in a solid will be discussed in chapter 2.

1.4. Connection to measurable quantities

1.4.1. Dynamical structure factor

In both *angular resolved electron energy loss spectroscopy (AR-EELS)* and *inelastic X-ray scattering (IXS)* the *double differential cross section* $\frac{\partial^2\sigma}{\partial\Omega\partial E}$ is measured. It quantifies the probability that an incoming particle (electron or photon, respectively) is scattered into the solid angle Ω and looses the energy E. If the incoming particle can be described with a single plane wave, the double differential cross section can be written in terms of the *dynamic structure factor S (DSF)* and the so-called *probe factor C*

$$\frac{\partial^2\sigma}{\partial\Omega\partial E} = C(\boldsymbol{q})S(\boldsymbol{q}, E), \tag{1.25}$$

where $\boldsymbol{q} = \boldsymbol{k}_\mathrm{i} - \boldsymbol{k}_\mathrm{f}$ is the difference in wave vector between the incoming and the scattered particle. The DSF is purely a property of the target material and thus it is independent of the scattering particle. Hence, both AR-EELS and IXS allow for the determination of the structure factor and only differ in the probe factors. When the incoming particle is instead described by a coherent sum of plane waves, eq. (1.25) can be generalized and the target properties are then described by the *mixed dynamic form factor $S(\boldsymbol{q}, \boldsymbol{q}', E)$* (MDFF). The *(generalized) fluctuation-dissipation theorem* now relates the (MDFF) DSF with the retarded density correlation function [1]:

$$S(\boldsymbol{q}, \boldsymbol{q}', E) = \frac{\mathrm{i}}{2\pi}\left[\chi^\mathrm{R}(\boldsymbol{q}, \boldsymbol{q}', E) - \left(\chi^\mathrm{R}(\boldsymbol{q}', \boldsymbol{q}, E)\right)^*\right], E > 0 \tag{1.26a}$$

$$S(\boldsymbol{q}, E) = S(\boldsymbol{q}, \boldsymbol{q}, E) = -\frac{1}{\pi}\Im\left[\chi^\mathrm{R}(\boldsymbol{q}, \boldsymbol{q}, E)\right], E > 0. \tag{1.26b}$$

The DSF can thus be connected to the microscopic dielectric function using eq. (1.16)

$$S(\boldsymbol{q}, \omega) = -\frac{1}{\pi}v^{-1}(\boldsymbol{q})\Im\left[\varepsilon^{-1}(\boldsymbol{q}, \boldsymbol{q}, \omega)\right]. \tag{1.27}$$

Another related quantity is the *electron energy loss function* $L(\boldsymbol{q}, \omega)$ which is defined as

$$L(\boldsymbol{q}, \omega) = -\Im\left[\varepsilon^{-1}(\boldsymbol{q}, \boldsymbol{q}, \omega)\right]. \tag{1.28}$$

1.4.2. Optical absorption spectrum

In the case of vanishing $\boldsymbol{q}$ the longitudinal dielectric function can also be used to describe the transversal response [6, 7]. We write (see eqs. (1.10), (1.11) and (1.13))

$$\varepsilon^{\alpha\beta}_\mathrm{TT}(\omega) := \lim_{q\to 0}\varepsilon^{\alpha\beta}_\mathrm{TT}(\boldsymbol{q}, \boldsymbol{q}, \omega) = \lim_{q\to 0}\varepsilon^{\alpha\beta}_\mathrm{LL}(\boldsymbol{q}, \boldsymbol{q}, \omega) = \lim_{q\to 0}\frac{q_\alpha\varepsilon(\boldsymbol{q}, \boldsymbol{q}, \omega)q_\beta}{|\boldsymbol{q}|^2}. \tag{1.29}$$

In experiments one generally measures an averaged response instead of the microscopic one. In order to account for this, we average the microscopic dielectric function over some mesoscopic volume and define the *macroscopic dielectric function ε_M* as

$$\left\langle\varepsilon^{\alpha\beta}_\mathrm{TT}\right\rangle(\omega) = \lim_{q\to 0}\frac{q_\alpha\left\langle\varepsilon\right\rangle(\boldsymbol{q}, \boldsymbol{q}, \omega)q_\beta}{|\boldsymbol{q}|^2} =: \lim_{q\to 0}\frac{q_\alpha\varepsilon_\mathrm{M}(\boldsymbol{q}, \omega)q_\beta}{|\boldsymbol{q}|^2}. \tag{1.30}$$

The imaginary part the macroscopic dielectric function $\Im\left[\varepsilon_{\mathrm{M}}(\omega)\right]$ is often equated with the *optical absorption spectrum* [8]. Following [9], this can be motivated when we consider the energy per unit time dissipated in the medium expressed via the induced current and the field within the medium

$$P(t) = \int \boldsymbol{j}^{\mathrm{ind}}(\boldsymbol{r}, t)\boldsymbol{E}(\boldsymbol{r}, t)\,\mathrm{d}^3 r\,. \tag{1.31}$$

We now make the assumption that the electric field in the medium is purely transversal and of a defined wave vector $\boldsymbol{q}$ and frequency ω, i.e.

$$\boldsymbol{E}(\boldsymbol{r}, t) = \hat{\boldsymbol{e}} E_0 \mathrm{e}^{\mathrm{i}(\boldsymbol{q}\boldsymbol{r}-\omega t)} + \text{c.c.}. \tag{1.32}$$

Additionally, we assume that the induced current has the same time and space dependence as the electric field and is linearly related to it:

$$\boldsymbol{j}^{\mathrm{ind}}(\boldsymbol{r}, t) = \sigma(\boldsymbol{q}, \omega)\hat{\boldsymbol{e}} E_0 \mathrm{e}^{\mathrm{i}(\boldsymbol{q}\boldsymbol{r}-\omega t)} + \text{c.c.}, \tag{1.33}$$

where σ defines the *transverse conductivity*. Under these assumptions, P is constant in time and proportional to the real part of σ

$$P \propto \left|E_0\right|^2 \sigma_1(\boldsymbol{q}, \omega). \tag{1.34}$$

Then using the Maxwell equations, σ and ε can be related, in particular the real part of σ is given in terms of the imaginary part of ε:

$$\sigma_1(\boldsymbol{q}, \omega) \propto \omega\varepsilon_2(\boldsymbol{q}, \omega). \tag{1.35}$$

Consequently, the features of the absorption spectrum are defined by those of the imaginary part of the dielectric function. For anisotropic materials, however, this connection cannot be drawn as directly.

1.5. Response of a crystalline system

In a periodic crystal with Born-von-Karman boundary condition, we can write the Fourier transform of eq. (1.12) in terms of the reciprocal lattice vectors $\boldsymbol{G}$ and the reciprocal unit cell vectors $\boldsymbol{q}$ as (see Appendix B)

$$\varphi^{\mathrm{ext}}_{\boldsymbol{G}}(\boldsymbol{q}, \omega) = \sum_{\boldsymbol{G}'} \varepsilon_{\boldsymbol{G}\boldsymbol{G}'}(\boldsymbol{q}, \boldsymbol{q}, \omega)\varphi_{\boldsymbol{G}'}(\boldsymbol{q}, \omega), \tag{1.36}$$

where we assume the response function to be lattice periodic $\varepsilon(\boldsymbol{r} + \boldsymbol{R}, \boldsymbol{r}' + \boldsymbol{R}) = \varepsilon(\boldsymbol{r}, \boldsymbol{r})$. Equation (1.36) highlights that even if the external potential is varying slowly, i.e. only Fourier coefficients with $\boldsymbol{G} = 0$ are non-zero, the resulting total potential varies on a small scale (it contains large $\boldsymbol{G}$ components). These deviations from the external potential are commonly referred to as *local field effects*, and the sum eq. (1.36) must be used to account for them.

Analogously, we can write for the inverse microscopic dielectric function

$$\varepsilon^{-1}_{\boldsymbol{G}\boldsymbol{G}'}(\boldsymbol{q},\omega) = 1 + v_{\boldsymbol{G}}(\boldsymbol{q})\chi^{\mathrm{R}}_{\boldsymbol{G}\boldsymbol{G}'}(\boldsymbol{q},\omega). \tag{1.37}$$

The dynamical structure factor for the momentum transfer $\boldsymbol{Q}_{\mathrm{mt}} = \boldsymbol{G}_{\mathrm{mt}} + \boldsymbol{q}_{\mathrm{mt}}$ takes on the form

$$S_{\boldsymbol{G}_{\mathrm{mt}}}(\boldsymbol{q}_{\mathrm{mt}},\omega) = -\frac{1}{\pi}v^{-1}_{\boldsymbol{G}_{\mathrm{mt}}}(\boldsymbol{q}_{\mathrm{mt}})\Im\left[\varepsilon^{-1}_{\boldsymbol{G}_{\mathrm{mt}}\boldsymbol{G}_{\mathrm{mt}}}(\boldsymbol{q}_{\mathrm{mt}},\boldsymbol{q}_{\mathrm{mt}},\omega)\right]. \tag{1.38}$$

1.5.1. Macroscopic dielectric response

For a crystalline system the mesocopic averaging mentioned in section 1.4.2 is usually done over the volume of a unit cell which is equivalent to taking only the $\boldsymbol{G} = 0$ component of the Fourier transform unequal to zero [10, 11]. Consequently, a macroscopic response function relates the $\boldsymbol{G} = 0$ components of two quantities. When we assume that the external potential is also macroscopic, i.e. $\varphi^{\mathrm{ext}}_{\boldsymbol{G}}(\boldsymbol{q}) = \delta_{\boldsymbol{G},0}\varphi^{\mathrm{ext}}(\boldsymbol{q})$, we find for the *macroscopic inverse longitudinal dielectric function* ε_M:

$$\varphi_0(\boldsymbol{q},\omega) = \varepsilon^{-1}_{00}(\boldsymbol{q},\boldsymbol{q},\omega)\varphi^{\mathrm{ext}}_0(\boldsymbol{q},\omega) =: \varepsilon^{-1}_{\mathrm{M}}(\boldsymbol{q},\omega)\varphi^{\mathrm{ext}}_0(\boldsymbol{q},\omega). \tag{1.39}$$

The equation above also allows for the definition of the *macroscopic longitudinal dielectric function* as

$$\varphi^{\mathrm{ext}}_0(\boldsymbol{q},\omega) = \frac{1}{\varepsilon^{-1}_{\mathrm{M}}(\boldsymbol{q},\omega)}\varphi_0(\boldsymbol{q},\omega) =: \varepsilon_{\mathrm{M}}(\boldsymbol{q},\omega)\varphi_0(\boldsymbol{q},\omega). \tag{1.40}$$

In view of eq. (1.27), we formally extend the definition of ε_{M} to also include the case of $\boldsymbol{G} \neq 0$

$$\varepsilon_{\mathrm{M}}(\boldsymbol{Q},\omega) = \frac{1}{\varepsilon^{-1}_{\boldsymbol{G}\boldsymbol{G}}(\boldsymbol{q},\omega)}. \tag{1.41}$$

Then we can write for the dynamical structure factor

$$S(\boldsymbol{Q},\omega) = -\frac{1}{\pi}v^{-1}_{\boldsymbol{G}}(\boldsymbol{q})\Im\left[\frac{1}{\varepsilon_{\mathrm{M}}(\boldsymbol{Q},\omega)}\right]. \tag{1.42}$$

For the limit of vanishing momentum transfer the macroscopic dielectric function can be most conveniently computed by introducing a modified polarizability $\bar{P}$ [8]

$$\bar{P} = P + P\bar{v}\bar{P}, \tag{1.43}$$

which is related to the polarizability P through the long-range-truncated Coulomb potential

$$\bar{v}_{\boldsymbol{G}}(\boldsymbol{q}) = \begin{cases} v_{\boldsymbol{G}}(\boldsymbol{q}) & \text{for} \quad \boldsymbol{G} \neq 0 \\ 0 & \text{otherwise} \end{cases}. \tag{1.44}$$

Using this approach we can take the limit $\boldsymbol{q} \to 0$ in eq. (1.16) and write

$$\varepsilon_M(\omega) = 1 - \lim_{q\to 0} v_0(\boldsymbol{q})\bar{P}_{00}(\boldsymbol{q},\omega). \tag{1.45}$$

2. The many-body problem in solid-state physics

In this chapter, we summarize some key concepts used in the *ab initio* quantum mechanical description of a solid as an electronic many-body system. First, the Hamiltonian for a general N-electron system is presented in section 2.1, as a starting point for the following discussions. Then, as an alternative approach to the problem, the main ideas and results of *density-functional theory* are presented in section 2.2. In section 2.3 the formalism of *Green's function theory* as a means to describe elementary excitations of the system and the *quasi-particle*-picture are introduced. In section 2.3.3 the one-particle Green's function, or propagator, and Hedin's equations are discussed. Subsequently, in section 2.3.4, the derivation of the *Bethe-Salpeter equation* (BSE) in the so-called *GW*-approximation for static screening is outlined starting from the two-particle propagator. Lastly, the diagrammatic representations of the BSE and the *Tamm-Dancoff-approximation* are discussed in section 2.3.5.

2.1. The electronic many-body system

The many electron system we are interested in is described by a Hamiltonian of the form

$$\hat{\mathrm{H}} = \hat{\mathrm{T}} + \hat{\mathrm{V}} + \hat{\mathrm{U}}, \tag{2.1}$$

where $\hat{\mathrm{T}}$ and $\hat{\mathrm{V}}$ are the summed one-particle operators describing the kinetic and potential energy of N electrons in an external potential, while $\hat{\mathrm{U}}$ contains the two-electron Coulomb repulsion terms. In atomic units the operators are given by

$$\hat{\mathrm{T}} = \sum_{i=1} \hat{\mathrm{t}}_i = -\frac{1}{2}\sum_{i=1} \nabla_i^2 \qquad \hat{\mathrm{V}} = \sum_{i=1} v_{\mathrm{ext}}(\boldsymbol{r}_i), \tag{2.2a}$$

$$\hat{\mathrm{U}} = \frac{1}{2}\sum_{i\neq j} v(\boldsymbol{r}_i, \boldsymbol{r}_j) = \sum_{i,j} \frac{1}{\left|\boldsymbol{r}_i - \boldsymbol{r}_j\right|} \qquad v_{\mathrm{ext}}(\boldsymbol{r}; \left\{\boldsymbol{R}_n\right\}) = -\sum_{i=1}^{N_{\mathrm{nuc}}} \frac{Z_i}{\left|\boldsymbol{r} - \boldsymbol{R}_i\right|}. \tag{2.2b}$$

The external potential v_{ext} is generated by the positively charged atomic nuclei which are assumed to be in a fixed arrangement. A direct solution of the full N-electron Schrödinger equation

$$\hat{\mathrm{H}}\Phi\left(\left\{\boldsymbol{r}_i\right\};\left\{\boldsymbol{R}_i\right\}\right) = \mathrm{i}\frac{\partial}{\partial t}\Phi\left(\left\{\boldsymbol{r}_i\right\};\left\{\boldsymbol{R}_i\right\}\right) \tag{2.3}$$

for any realistic system is not feasible due to its high dimensionality[1]. This problem is lifted in the framework of density-functional theory.

---

[1] A 1 cm^3 cube of silicon contains about 10^{23} electrons

2.2. Density-functional theory

In the context of density-functional theory, pioneered by the works of Thomas [12] and Fermi [13] and formalized by Hohenberg and Kohn [14], the focus is shifted away from the many-electron wave-function onto the electron density as the quantity describing the system.

2.2.1. Hohenberg-Kohn theorems

The theory is founded on the so called *Hohenberg-Kohn theorem* that states [14]:

Theorem 1. *There is a one-to-one correspondence between the ground state electron density of a bound system of interacting electrons and the external potential.*

Corollary 1.1. *Every observable and the wave-function of the system can be expressed as a functional of the ground state density.*

In particular, the sum of the electron-electron Coulomb interaction $\hat{\mathrm{U}}$ and the kinetic energy of the electrons $\hat{\mathrm{T}}$

$$F[n] = \langle \Phi | \hat{\mathrm{T}} + \hat{\mathrm{U}} | \Phi \rangle \tag{2.4}$$

is uniquely defined by the ground state density and has the *same form for all many-electron systems* of the considered form.

The second theorem of Hohenberg and Kohn, also known as *Hohenberg-Kohn minimum principle*, states:

Theorem 2. *The total energy is a functional of the electron density with its minimal value, the ground state energy, at the ground state density*

$$E_{gs} = E[n_{gs}] = \min_{n(\boldsymbol{r})} E[n(\boldsymbol{r})] = \min_{n(\boldsymbol{r})} \left\{ \int n(\boldsymbol{r}) v_{ext}(\boldsymbol{r}) \, \mathrm{d}^3 r + F[n] \right\}. \tag{2.5}$$

2.2.2. The Kohn-Sham equations

While in theory every observable of the N-electron system is a functional of the density, the explicit form of $F[n]$ is not known. In an effort to make the problem more tractable, Kohn and Sham [15] expressed the universal functional as

$$F[n(\boldsymbol{r})] = T_0[n(\boldsymbol{r})] + \frac{1}{2} \iint \frac{n(\boldsymbol{r}_1) n(\boldsymbol{r}_2)}{|\boldsymbol{r}_1 - \boldsymbol{r}_2|} \, \mathrm{d}^3 r_1 \, \mathrm{d}^3 r_2 + E_{\mathrm{xc}}[n(\boldsymbol{r})], \tag{2.6}$$

where $T_0[n]$ is the kinetic energy functional of *non-interacting* electrons, the second summand is the electrostatic Hartee-energy and $E_{\mathrm{xc}}[n]$ is the *exchange-correlation energy functional*. The latter encapsulates all quantum-mechanical many-body effects and needs to be approximated.

By applying the Hohenberg-Kohn minimum principle Kohn and Sham were able to define an *auxiliary system of non-interacting electrons that leads to the exact same ground-state density as the fully interacting system*, given the exact form of the exchange-correlation energy functional:

$$\left[-\frac{1}{2}\nabla^2 + v_{\mathrm{eff}}(\boldsymbol{r}) - \epsilon_i\right]\phi_i(\boldsymbol{r}) =: \hat{\mathrm{h}}_{\mathrm{KS}}(\boldsymbol{r})\phi_i(\boldsymbol{r}) = 0, \tag{2.7a}$$

where

$$v_{\mathrm{eff}}(\boldsymbol{r}) = v_{\mathrm{ext}}(\boldsymbol{r}) + \int \frac{n(\boldsymbol{r}_2)}{|\boldsymbol{r} - \boldsymbol{r}_2|}\,\mathrm{d}^3 r_2 + v_{\mathrm{xc}}(\boldsymbol{r}) \tag{2.7b}$$

and

$$v_{\mathrm{xc}}(\boldsymbol{r}) = \left.\frac{\delta E_{\mathrm{xc}}[n(\boldsymbol{r})]}{\delta n(\boldsymbol{r})}\right|_{n=n_{\mathrm{gs}}}. \tag{2.7c}$$

Equation (2.7c) defines the *exchange-correlation potential.* The electron density can be directly calculated using the single-particle orbitals

$$n(\boldsymbol{r}) = \sum_{i=1}^{N} |\phi_i(\boldsymbol{r})|, \tag{2.8}$$

and the total energy reads in terms of the density and the Kohn-Sham eigenvalues

$$E = \sum_{i=1}^{N}\epsilon_i + E_{\mathrm{xc}}[n(\boldsymbol{r})] - \int v_{\mathrm{xc}}(\boldsymbol{r})n(\boldsymbol{r})\,\mathrm{d}^3 r - \frac{1}{2}\int \frac{n(\boldsymbol{r}_1)n(\boldsymbol{r}_2)}{|\boldsymbol{r}_1 - \boldsymbol{r}_2|}\,\mathrm{d}^3 r_1\,\mathrm{d}^3 r_2\,. \tag{2.9}$$

Starting from an assumed form of $E_{\mathrm{xc}}[n]$, equations (2.7), (2.8) and (2.9) need to be solved self-consistently for the ground-state density.

Remark. The Kohn-Sham eigenvalues and Kohn-Sham orbitals contain *a priori* no physical meaning, as they are auxiliary quantities designed to reproduce the ground state electron density of the real system. In practice, however, they are still used to approximate band structures and wave functions and often yield reasonable results when compared with experiments and higher order theories.

In principle, all many-body effects of the interacting system are described in the exchange-correlation energy functional, and consequently the Kohn-Sham system with the corresponding exchange-correlation potential can reproduce the exact ground state density and energy. Unfortunately, the exact form of the functional is not known and approximations need to be made. In this work we will exclusively use the *local density approximation* (LDA) [15] which assumes the system to locally resemble the homogeneous electron gas.

2.3. Many-body perturbation theory

If one is interested in the excitation properties of a system of interacting electrons it does not suffice to look at the Kohn-Sham eigenvalues, as they are purely auxiliary quantities. Instead one has to venture into the realm of many-body perturbation theory (MBPT) within the (non-relativistic) second quantization formulation of the many-electron system (for a review see [8, 16]). In this section, the basic concepts will be outlined following mainly Refs. [2, 10, 11, 16].

2.3.1. Hamiltonian in second quantization

In MBPT it is necessary to switch to the occupation number representation of the second quantization formalism. The system described by eq. (2.1) now reads

$$\hat{\mathrm{H}} = \int \hat{\Psi}^{\dagger}(\boldsymbol{r}) h(\boldsymbol{r}) \hat{\Psi}(\boldsymbol{r}) \, \mathrm{d}^3 r + \frac{1}{2} \iint \hat{\Psi}^{\dagger}(\boldsymbol{r}) \hat{\Psi}^{\dagger}(\boldsymbol{r}') v(\boldsymbol{r}, \boldsymbol{r}') \hat{\Psi}(\boldsymbol{r}') \hat{\Psi}(\boldsymbol{r}) \, \mathrm{d}^3 r \, \mathrm{d}^3 r' \, . \tag{2.10}$$

The fermionic field operators $\hat{\Psi}^{\dagger}(\boldsymbol{r})$ and $\hat{\Psi}(\boldsymbol{r})$ create and destroy an electron at position $\boldsymbol{r}$, respectively, and fulfill the equal-time anti-commutation relations

$$\left[\hat{\Psi}(\boldsymbol{r}), \hat{\Psi}(\boldsymbol{r}')\right]_+ = \left[\hat{\Psi}^{\dagger}(\boldsymbol{r}), \hat{\Psi}^{\dagger}(\boldsymbol{r}')\right]_+ = 0 \quad \text{and} \quad \left[\hat{\Psi}(\boldsymbol{r}), \hat{\Psi}^{\dagger}(\boldsymbol{r}')\right]_+ = \delta(\boldsymbol{r} - \boldsymbol{r}'). \tag{2.11}$$

Instead of the Schrödinger equation (2.3), the equation of motion of the field operators in the Heisenberg picture is considered to describe the evolution of the system

$$\mathrm{i}\frac{\partial}{\partial t} \hat{\Psi}_{\mathrm{H}}(\boldsymbol{r}, t) = \left[\hat{\Psi}_{\mathrm{H}}(\boldsymbol{r}, t), \hat{\mathrm{H}}\right] = \left[\hat{\mathrm{h}}(\boldsymbol{r}) + \int v(\boldsymbol{r}, \boldsymbol{r}') \hat{\Psi}^{\dagger}_{\mathrm{H}}(\boldsymbol{r}', t) \hat{\Psi}_{\mathrm{H}}(\boldsymbol{r}', t) \, \mathrm{d}^3 r'\right] \hat{\Psi}_{\mathrm{H}}(\boldsymbol{r}, t). \tag{2.12}$$

The direct solution of eq. (2.12) is in general not possible so that perturbative methods need to be employed.

2.3.2. Quasi-particles

The key concept of MBPT is to replace the system of N strongly interacting particles with a system of N non- or weakly interacting *quasi-particles* that describe elementary excitations of the system with respect to some perturbation. When considering (inverse) photoemission experiments where electrons are (added) removed from the system, an appropriate quasi-particle picture would be that of *quasi-electrons* (*quasi-holes*). These quasi-particles closely resemble the real particles, but with properties such as charge, mass or momentum renormalized by the influence of all the other electrons in the system. On the other hand, in optical absorption measurements excitations remain charge neutral and can be described by the creation of electron-hole pairs. These pairs of correlated electrons and holes can be characterized as a new quasi-particle called *exciton*. The theoretical description of these quasi-particle is bases on the *n-particle Green's functions* (or propagators). They give a systematical approach to the interaction of a few particles with the rest of the fully interacting system.

2.3.3. One-particle Green's function and Hedin's equations

The *one-particle Green's function* [5]

$$G_1(\boldsymbol{r}_1, t_1; \boldsymbol{r}_2, t_2) = -\mathrm{i} \langle N | \hat{\mathscr{T}} \left[\hat{\Psi}(\boldsymbol{r}_1, t_1) \hat{\Psi}^{\dagger}(\boldsymbol{r}_2, t_2)\right] | N \rangle \tag{2.13}$$

can be interpreted as a measure for the probability of finding a particle at position $\boldsymbol{r}$ at time t, if a particle is introduced into the system at position $\boldsymbol{r}'$ at time t'. Here, $|N\rangle$ is the Heisenberg ground state of the many-body system and $\hat{\mathscr{T}}$ is Wick's time-ordering operator. This Green's function contains all information about single-particle excitations of the system, and the expectation values of any single-particle observables can be computed with its help [5, 17]. Using functional-derivative methods [18–20], the interacting Green's function G_1 can be formulated in terms of the *non-interacting* Green's function G_0 and the *self-energy* Σ

$$G_0^{-1}(1,2) = G_1^{-1}(1,2) + \Sigma(1,2), \tag{2.14a}$$

$$G_1(1,2) = G_0(1,2) + \int G_0(1,3)\Sigma(3,4)G_1(4,2)\,\mathrm{d}(3,4)\,, \tag{2.14b}$$

where $1 \equiv (\boldsymbol{r}_1, t_1)$. G_0 describes the free propagation of a particle in the average electrostatic potential of the system, while exchange and correlation effects are packed into Σ. In order to get access to the self-energy, Hedin and Lundquist [2, 21] investigated the equation of motion of $G_1(1,2)$ for a Hamiltonian that is perturbed by a small local external scalar potential ϕ ($h(r) \to h(r)+\phi(r,t)$ in eq. (2.10)) and derived the following set of self-consistent integral equations, commonly referred to as *Hedin's equations*:

$$\Sigma(1,2) = \mathrm{i}\int W(1^+,3)G_1(1,4)\Gamma(4,2;3)\,\mathrm{d}(3,4) \tag{2.15a}$$

$$W(1,2) = v(1,2) + \int W(1,3)P(3,4)v(4,2)\,\mathrm{d}(3,4) \tag{2.15b}$$

$$P(1,2) = -\mathrm{i}\int G_1(2,3)G_1(4,2)\Gamma(3,4;1)\,\mathrm{d}(3,4) \tag{2.15c}$$

$$\Gamma(1,2;3) = \delta(1,2)\delta(1,3) + \frac{\delta\Sigma(1,2)}{\delta V(3)}. \tag{2.15d}$$

W denotes the *dynamically screened Coulomb interaction*, which is related to the *bare Coulomb interaction* v by the inverse (longitudinal) dielectric function ε^{-1}, according to:

$$W(1,2) = \int v(1,3)\varepsilon^{-1}(3,2)\,\mathrm{d}(3)\,. \tag{2.16}$$

The inverse of the dielectric function in eq. (2.16) is defined as the variation of the total average potential V of the system with respect to a scalar potential Φ (see section 1.2),

$$\varepsilon^{-1}(1,2) = \frac{\delta V(1)}{\delta\Phi(2)}. \tag{2.17}$$

Dyson's equation for G_1 (2.14) together with Hedin's equations (2.15) could be solved self-consistently starting with $\Sigma = 0$. In practice, however, this is computationally not feasible for realistic systems.

In order to make the system (2.15) tractable, the *vertex function* Γ is approximated by neglecting the variation of the self-energy with respect to the average potential V. The resulting system

$$\Sigma(1,2) = \mathrm{i}W(1^+,2)G_1(1,2) \tag{2.18a}$$

$$W(1,2) = v(1,2) + \int W(1,3)P(3,4)v(4,2)\,\mathrm{d}(3,4) \tag{2.18b}$$

$$P(1,2) = -\mathrm{i}G_1(1,2)G_1(2,1) \tag{2.18c}$$

is named the *GW approximation* due to the form of the self-energy. To further simplify the problem, the G_0W_0 approximation is often used, where the self-energy is approximated by one iteration of eq. (2.18) starting from G_0.

The Dyson equation eq. (2.14) can be reformulated in terms of the *quasi-particle wave functions* ψ as a Schrödinger-like equation

$$\hat{\mathrm{h}}(\boldsymbol{r})\psi_m(\boldsymbol{r}) + \int \Sigma(\boldsymbol{r},\boldsymbol{r}',E_m)\psi_m(\boldsymbol{r}')\,\mathrm{d}^3r' = E_m\psi_m(\boldsymbol{r}) \tag{2.19}$$

with the self energy considered as a non-local, energy-dependent potential [2, 22, 23]. The Green's function ($T = 0\,\mathrm{K}$) can be expressed in analogy to the independent-particle propagator using the solutions of eq. (2.19) as

$$G_1(\boldsymbol{r},\boldsymbol{r}',\omega) = \sum_m \frac{\psi_m(\boldsymbol{r})\psi_m^*(\boldsymbol{r}')}{\omega - E_m + \mathrm{i}\delta\,\mathrm{sgn}(E_m - E_\mathrm{f})}. \tag{2.20}$$

2.3.4. Two-particle Green's function and the Bethe-Salpether equation

To describe the perturbation discussed in chapter 1 in terms of Green's functions we also need to introduce the *two-particle Green's function*

$$\begin{aligned} &G_2(\boldsymbol{r}_1,t_1,\boldsymbol{r}_2,t_2;\boldsymbol{r}_1',t_1',\boldsymbol{r}_2',t_2') \\ &\quad = (-\mathrm{i})^2\,\langle N|\hat{\mathscr{T}}\left[\hat{\Psi}_\mathrm{H}(\boldsymbol{r}_1,t_1)\hat{\Psi}_\mathrm{H}(\boldsymbol{r}_2,t_2)\hat{\Psi}^\dagger_\mathrm{H}(\boldsymbol{r}_2',t_2')\hat{\Psi}^\dagger_\mathrm{H}(\boldsymbol{r}_1',t_1')\right]|N\rangle, \end{aligned} \tag{2.21}$$

which describes the propagation of two particles through the system. Now, the time-ordered density correlation function (1.23) can be expressed with G_1 and G_2 by using $\hat{\mathrm{n}}_\mathrm{H}(r,t) = \hat{\Psi}^\dagger_\mathrm{H}(r,t)\hat{\Psi}_\mathrm{H}(r,t)$ as

$$\chi^\mathrm{T}(1,2) = \mathrm{i}\left[G_2(1,2,1^+,2^+) - G_1(1,1^+)G_1(2,2^+)\right] = -\mathrm{i}L(1,2,1^+,2^+), \tag{2.22}$$

where L denotes the *two-particle correlation function* [24] which is defined by

$$L(1,2,1',2') = G_2(1,2,1',2') - G_1(1,1')G_1(2,2'). \tag{2.23}$$

The equation of motion of L is described by the *Bethe-Salpeter equation for L* in the form of a Dyson's equation

$$\begin{aligned} L(1,2,1',2') &= L_0(1,2;1',2') \\ &\quad + \int L_0(1,4;1',3)\Xi(3,5;4,6)L(6,2;5,2')\,\mathrm{d}(3,4,5,6)\,. \end{aligned} \tag{2.24}$$

Here, L_0 describes the independent propagation of two particles

$$L_0(1,2;1',2') = G_1(1,2')G_1(2,1'), \tag{2.25}$$

and the effective two-particle interaction kernel Ξ is given in terms of the variation of the irreducible self-energy Σ (see 2.3.3) and the Hartree part of the self energy Σ_{H},

$$\Sigma_{\mathrm{H}}(3,4) = -\mathrm{i}\delta(3,4)\int \mathrm{d}(5)\,v(1,5)G_1(3,3^+) \tag{2.26}$$

with respect to the one-particle Green's function

$$\Xi(3,5;4,6) = \frac{\delta\left(\Sigma_{\mathrm{H}}(3,4)+\Sigma(3,4)\right)}{\delta G_1(6,5)}. \tag{2.27}$$

In the following, we will focus on the description of electron-hole pairs and exclude electron-electron or hole-hole pairs by requiring that $t_1 = t_1'$ and $t_2 = t_2'$. That is, we are only interested in charge-neutral excitations. In this framework L_0, for example, describes the *independent* propagation of an electron and a hole through the system and is only dependent on one time difference $t_2 - t_1$ [16].

Choosing the GW-approximation for the self-energy (2.18), the functional-derivative (2.27) is evaluated to yield:

$$\begin{aligned} \Xi(3,5,4,6) &= -\mathrm{i}\delta(3,4)\delta(5,6)v(3,6) + \mathrm{i}\delta(3,6)\delta(4,5)W(3,5) \\ &\quad + \mathrm{i}G_1(3,5)\frac{\delta W(3,5)}{\delta G_1(6,4)}. \end{aligned} \tag{2.28}$$

The first term in eq. (2.28) describes the *repulsive exchange interaction*, while the second one accounts for the *screened electron-hole attraction*. The last term is neglected in practical applications, meaning that no change of the screening due to the excitations is considered.

To make the Bethe-Salpeter equation computationally more tractable, we approximate the interaction kernel (2.28) further by assuming that the screening is frequency independent, i.e. static, and all interactions are instantaneous

$$\begin{aligned} \Xi(3,5,4,6) &\approx -\mathrm{i}\delta(3,4)\delta(5,6)v(\boldsymbol{r}_3,\boldsymbol{r}_6)\delta(t_3-t_6) \\ &\quad + \mathrm{i}\delta(3,6)\delta(4,5)W(\boldsymbol{r}_3,\boldsymbol{r}_5)\delta(t_3-t_5). \end{aligned} \tag{2.29}$$

This entails that the Fourier transform of the kernel in this approximation is *frequency-independent*, i.e. $\Xi(\omega) = \Xi$.

Once the BSE is solved for L, the density correlation function can be expressed using eq. (2.22). Form this function one can extract the dielectric response of the system which accounts for excitonic effects (see chapter 1).

2.3.5. BSE in diagrams

The integral equation (2.24) can be visualized in terms of Feynman diagrams according to

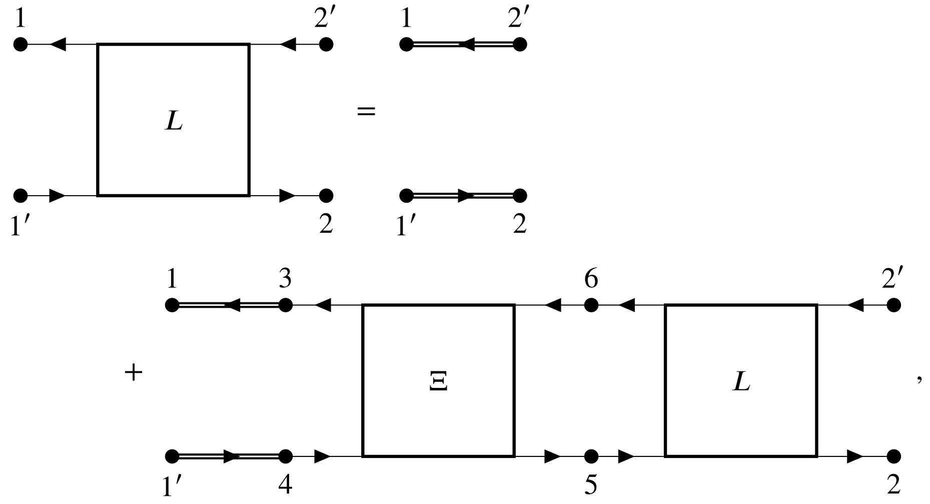

(2.30)

where we used the “box with four tails” notation of the four-point functions and we denote the quasi-particle propagator as $G(2,1) =$ 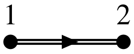 . The tails are not associated with any propagators but define how to connect propagators to the four-point function. The approximation for the interaction kernel Ξ (2.29) can be written diagrammatically as

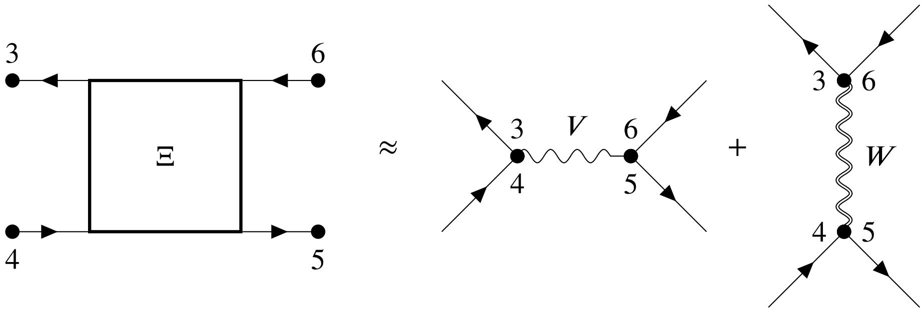

(2.31)

and the screened Coulomb interaction itself is given by the Dyson equation in terms of the irreducible polarization P

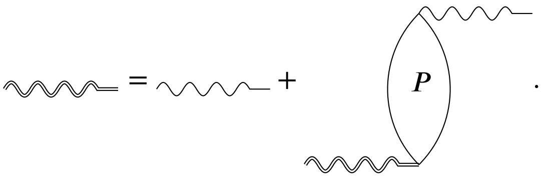

(2.32)

In the following, we will approximate P as

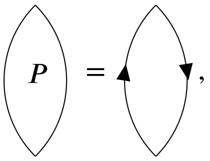

(2.33)

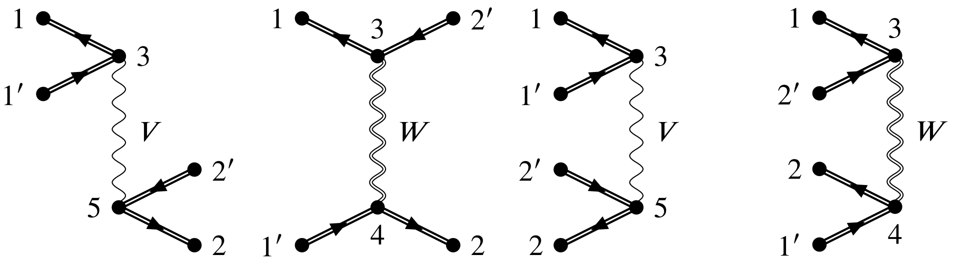

(a) (b) (c) (d)

Figure 2.1.: First-order time-ordered Goldstone diagrams corresponding to the interactions mitigated by the bare (V) and the screened (W) Coulomb potential in the BSE (2.30) with the two-particle interaction kernel (2.31). Time increases from left to right. Diagrams (a) and (b) describe the resonant-resonant coupling between the e-h pairs ($11'$) and ($22'$), where both are associated with the frequency ω. Diagrams (c) and (d) describe the resonant-anti-resonant coupling, in which the ($22'$) pair is associated with the frequency of opposite sign. See also [26].

which is commonly referred to as *random phase approximation* (RPA) [25].

It is instructive to look at the time-ordered Goldstone versions of the first order interaction processes in eq. (2.30) with the kernel (2.31) as shown in figure 2.1. In the exchange diagram (a) the incoming electron-hole (e-h) pair ($11'$) is annihilated at $(\boldsymbol{r}_3, t_3)$ and the outgoing e-h pair ($22'$) is created at $(\boldsymbol{r}_5, t_3)$ with the same associated frequency ω. In contrast, in diagram (c) the incoming resonant e-h pair annihilates with an anti-resonant e-h pair of opposite frequency. Diagram (b) describes the scattering of the incoming resonant e-h pair into another resonant e-h pair of the same frequency. Lastly, in diagram (d) the incoming resonant e-h pair scatters into an anti-resonant e-h pair of opposite frequency.

A common approximation to the BSE is the so-called *Tamm-Dancoff approximation*, where no coupling between resonant and anti-resonant e-h pairs is regarded, i.e. diagrams of the type (c) and (d) are neglected. Within the TDA there is only one electron-hole pair present at any given time, whereas any number of electron-hole pairs are permitted otherwise [5].

3. Solving the Bethe-Salpeter equation

In this chapter we discuss how to bring the BSE into a numerically accessible form. In section 3.1 the integral equation (2.24) is written in matrix notation by expanding all functions in terms of a two-particle basis. Then, the formulation of the BSE is specialized for crystalline systems in section 3.2 and the explicit expressions of the momentum-transfer dependent matrix elements are derived in section 3.3. Subsequently, in sections 3.4 to 3.6 the connection between the eigen-solutions of an effective two-particle Hamiltonian and the reducible polarization function is made. Finally, in section 3.7 the computation of the macroscopic dielectric tensor in the limit of vanishing momentum transfer is discussed.

3.1. Matrix form of the BSE

We start by defining the four-point extension of the time-ordered density-correlation function eq. (2.22) as

$$\chi(1,2,1',2') \coloneqq -\mathrm{i}L(1,2,1',2'), \tag{3.1}$$

where $\chi(1,2) = \chi(1,2,1,2)$. Then, using the approximate (static) interaction kernel (2.29), the BSE eq. (2.24) can be Fourier transformed in the time difference $t_2 - t_1$ resulting in

$$\begin{aligned}\chi(\boldsymbol{r}_1,\boldsymbol{r}_2,\boldsymbol{r}'_1,\boldsymbol{r}'_2,\omega) &= \chi_0(\boldsymbol{r}_1,\boldsymbol{r}_2,\boldsymbol{r}'_1,\boldsymbol{r}'_2,\omega)\\ &+ \int \chi_0(\boldsymbol{r}_1,\boldsymbol{r}_4,\boldsymbol{r}'_1,\boldsymbol{r}_3,\omega)\Xi(\boldsymbol{r}_3,\boldsymbol{r}_5,\boldsymbol{r}_4,\boldsymbol{r}_6)\chi(\boldsymbol{r}_6,\boldsymbol{r}_2,\boldsymbol{r}_5,\boldsymbol{r}'_2,\omega)\,\mathrm{d}^3r_3\,\mathrm{d}^3r_4\,\mathrm{d}^3r_5\,\mathrm{d}^3r_6\,.\end{aligned} \tag{3.2}$$

With the independent quasi-particle approximation of the one-particle Green's function eq. (2.20), the Fourier transform of $\chi_0 = -\mathrm{i}L_0$ eq. (2.25) takes on the form (see Appendix F)

$$\chi_0(\boldsymbol{r}_1,\boldsymbol{r}_2,\boldsymbol{r}'_1,\boldsymbol{r}'_2,\omega) = \sum_{o,u} \frac{\psi_o(\boldsymbol{r}_1)\psi^*_u(\boldsymbol{r}'_1)\psi^*_o(\boldsymbol{r}'_2)\psi_u(\boldsymbol{r}_2)}{\omega-(\varepsilon_u-\varepsilon_o)+\mathrm{i}\delta} + \frac{\psi_u(\boldsymbol{r}_1)\psi^*_o(\boldsymbol{r}'_1)\psi^*_u(\boldsymbol{r}'_2)\psi_o(\boldsymbol{r}_2)}{-\omega-(\varepsilon_u-\varepsilon_o)+\mathrm{i}\delta}. \tag{3.3}$$

Equation (3.3) suggests the introduction of a two-particle basis $\Upsilon_j(\boldsymbol{r},\boldsymbol{r}')$ that is split into two subspaces according to

$$\Upsilon^{\mathrm{r}}_\alpha(\boldsymbol{r},\boldsymbol{r}') = \psi_{o_\alpha}(\boldsymbol{r})\psi^*_{u_\alpha}(\boldsymbol{r}') \quad \text{and} \quad \Upsilon^{\mathrm{a}}_\alpha(\boldsymbol{r},\boldsymbol{r}') = \psi_{u_\alpha}(\boldsymbol{r})\psi^*_{o_\alpha}(\boldsymbol{r}'). \tag{3.4}$$

The superscripts r and a denote the resonant and anti-resonant subspaces respectively, and the subscript α labels a combination of one unoccupied and one unoccupied state. In other words, α labels the independent (quasi-)particle transitions. Resonat (anti-resonant) refers here to the part of χ_0 that has poles when ω is positive (negative).

By restricting the one-particle Hilbert space to the span of a finite number of N_{o} occupied and N_{u} unoccupied orbitals, the Bethe-Salpeter equation (3.2) can be written as a matrix equation in the two-particle basis (3.4):

$$\chi_{ij}(\omega) = \chi_{0ij}(\omega) + \sum_{kl} \chi_{0ik}(\omega) \underbrace{\left(V_{kl} - W_{kl}\right)}_{\Xi_{kl}} \chi_{lj}(\omega). \tag{3.5}$$

Using the basis functions of (3.4), the matrix elements of the kernel are computed according to the prescription

$$\Xi^{\mathrm{rr}}_{\alpha\alpha'} = \iiiint \Upsilon^{\mathrm{r}*}_{\alpha}(\boldsymbol{r}_1, \boldsymbol{r}_1')\Xi(\boldsymbol{r}_1, \boldsymbol{r}_2, \boldsymbol{r}_1', \boldsymbol{r}_2')\Upsilon^{\mathrm{r}}_{\alpha'}(\boldsymbol{r}_2', \boldsymbol{r}_2)\, \mathrm{d}^3 r_1\, \mathrm{d}^3 r_1'\, \mathrm{d}^3 r_2\, \mathrm{d}^3 r_2', \tag{3.6}$$

and the ra-, ar- and aa-blocks are computed analogously. In this notation, the exchange part of Ξ is

$$\Xi_v(\boldsymbol{r}_1, \boldsymbol{r}_2, \boldsymbol{r}_1', \boldsymbol{r}_2') = \delta(\boldsymbol{r}_1 - \boldsymbol{r}_1')\delta(\boldsymbol{r}_2 - \boldsymbol{r}_2')v(\boldsymbol{r}_1, \boldsymbol{r}_2) \tag{3.7}$$

while the screened Coulomb interaction takes of the form

$$\Xi_w(\boldsymbol{r}_1, \boldsymbol{r}_2, \boldsymbol{r}_1', \boldsymbol{r}_2') = -\delta(\boldsymbol{r}_1 - \boldsymbol{r}_2')\delta(\boldsymbol{r}_1' - \boldsymbol{r}_2)W(\boldsymbol{r}_1, \boldsymbol{r}_2). \tag{3.8}$$

The solution of the integral equation (3.2) is thus mapped to the linear algebra problem

$$\boldsymbol{\chi} = \left[\chi_0^{-1}(\omega) - \Xi\right]^{-1}. \tag{3.9}$$

3.2. BSE for crystalline systems

In a crystalline system, χ follows the periodicity of the lattice

$$\chi(\boldsymbol{r}_1 + \boldsymbol{R}, \boldsymbol{r}_2 + \boldsymbol{R}, \boldsymbol{r}_1' + \boldsymbol{R}, \boldsymbol{r}_2' + \boldsymbol{R}, \omega) = \chi(\boldsymbol{r}_1, \boldsymbol{r}_2, \boldsymbol{r}_1', \boldsymbol{r}_2', \omega) \tag{3.10}$$

and can be expressed in terms of a sum of functions defined for each point in the Brillouin zone [10]

$$\chi(\boldsymbol{r}_1, \boldsymbol{r}_2, \boldsymbol{r}_1', \boldsymbol{r}_2', \omega) = \sum_{\boldsymbol{q}_{\mathrm{mt}} \in \mathrm{B.z.}} \chi_{\boldsymbol{q}_{\mathrm{mt}}}(\boldsymbol{r}_1, \boldsymbol{r}_2, \boldsymbol{r}_1', \boldsymbol{r}_2', \omega). \tag{3.11}$$

Since the one-particle wave functions are Bloch functions, also the two-particle basis functions can be chosen to be Bloch-periodic in $\boldsymbol{q}_{\mathrm{mt}}$. We define the resonant and anti-resonant basis functions as

$$\Upsilon^{\mathrm{r}}_{\alpha,\boldsymbol{q}_{\mathrm{mt}}}(\boldsymbol{r}, \boldsymbol{r}') = \psi_{o_\alpha \boldsymbol{k}_\alpha + \boldsymbol{q}_{\mathrm{mt}}/2}(\boldsymbol{r})\psi^*_{u_\alpha \boldsymbol{k}_\alpha - \boldsymbol{q}_{\mathrm{mt}}/2}(\boldsymbol{r}') \tag{3.12a}$$

and

$$\Upsilon^{\mathrm{a}}_{\alpha,\boldsymbol{q}_{\mathrm{mt}}}(\boldsymbol{r}, \boldsymbol{r}') = \psi_{u_\alpha \boldsymbol{k}_\alpha + \boldsymbol{q}_{\mathrm{mt}}/2}(\boldsymbol{r})\psi^*_{o_\alpha \boldsymbol{k}_\alpha - \boldsymbol{q}_{\mathrm{mt}}/2}(\boldsymbol{r}'). \tag{3.12b}$$

It is now possible to solve eq. (3.5) for each $\boldsymbol{q}_{\mathrm{mt}}$ component separately by restricting the two-particle basis according to eq. (3.12), i.e.

$$\boldsymbol{\chi}(\boldsymbol{q}_{\mathrm{mt}}, \omega) = \left[\boldsymbol{\chi}_0^{-1}(\boldsymbol{q}_{\mathrm{mt}}, \omega) - \Xi(\boldsymbol{q}_{\mathrm{mt}})\right]^{-1}. \tag{3.13}$$

In the following we approximate the quasi-particle states $\psi_{i,\boldsymbol{k}}$ with the Kohn-Sham orbitals $\phi_{i,\boldsymbol{k}}$. For diamond, Si, Ge, and LiCl this is known to be a good approximation [23]. Changing the enumeration of the $\boldsymbol{k}$ points in the definition of the anti-resonant part of the two-particle basis according to

$$\Upsilon^{\bar{\mathrm{a}}}_{\alpha,\boldsymbol{q}_{\mathrm{mt}}}(\boldsymbol{r},\boldsymbol{r}') = \phi_{u_\alpha - \boldsymbol{k}_\alpha + \boldsymbol{q}_{\mathrm{mt}}/2}(\boldsymbol{r}), \phi^*_{o_\alpha - \boldsymbol{k}_\alpha - \boldsymbol{q}_{\mathrm{mt}}/2}(\boldsymbol{r}') \tag{3.14}$$

is useful when considering the symmetry properties of the Bloch states under time-reversal

$$\phi_{\boldsymbol{k}} = \phi^*_{-\boldsymbol{k}} \quad \text{and} \quad \varepsilon_{\boldsymbol{k}} = \varepsilon_{-\boldsymbol{k}} \tag{3.15}$$

(see Appendix A.3.2). In this way, there is a direct connection between the resonant and anti-resonant basis functions [26]

$$\begin{aligned}\Upsilon^{\bar{\mathrm{a}}}_{\alpha,\boldsymbol{q}_{\mathrm{mt}}}(\boldsymbol{r},\boldsymbol{r}') &= \phi_{u_\alpha - \boldsymbol{k}_\alpha + \boldsymbol{q}_{\mathrm{mt}}/2}(\boldsymbol{r})\phi^*_{o_\alpha - \boldsymbol{k}_\alpha - \boldsymbol{q}_{\mathrm{mt}}/2}(\boldsymbol{r}') \\ &= \phi_{o_\alpha \boldsymbol{k}_\alpha + \boldsymbol{q}_{\mathrm{mt}}/2}(\boldsymbol{r}')\phi^*_{u_\alpha \boldsymbol{k}_\alpha - \boldsymbol{q}_{\mathrm{mt}}/2}(\boldsymbol{r}) = \Upsilon^{\mathrm{r}}_{\alpha,\boldsymbol{q}_{\mathrm{mt}}}(\boldsymbol{r}',\boldsymbol{r}).\end{aligned} \tag{3.16}$$

3.3. Matrix elements

In this section, the explicit form of the matrix elements needed for $\chi(\boldsymbol{q}_{\mathrm{mt}},\omega)$ (3.13) in the two-particle Bloch basis functions are given. The matrix representation of an operator $\hat{\mathrm{O}}$ has the block structure

$$\mathbf{O} = \begin{pmatrix} \mathbf{O}^{\mathrm{rr}} & \mathbf{O}^{\mathrm{ra}} \\ \mathbf{O}^{\mathrm{ar}} & \mathbf{O}^{\mathrm{aa}} \end{pmatrix}, \tag{3.17}$$

where the superscripts corresponds to the subspaces. In the following, we also adapt the notational convention for matrix elements in terms of the single-particle states

$$\langle m,n|\hat{\mathrm{O}}|i,j\rangle = \iint \phi^*_m(\boldsymbol{r})\phi^*_n(\boldsymbol{r}')O(\boldsymbol{r},\boldsymbol{r}')\phi_i(\boldsymbol{r})\phi_j(\boldsymbol{r}')\,\mathrm{d}^3r\,\mathrm{d}^3r'\,. \tag{3.18}$$

To shorten the notation in the following we write

$$\boldsymbol{k}_+ = \boldsymbol{k} + \boldsymbol{q}_{\mathrm{mt}}/2 \quad \text{and} \quad \boldsymbol{k}_- = \boldsymbol{k} - \boldsymbol{q}_{\mathrm{mt}}/2. \tag{3.19}$$

3.3.1. Independent-particle polarization function

The matrix elements of χ_0 are straightforwardly computed using eq. (3.3) and eq. (3.6). In the subsequent discussion, we will drop the infinitesimal δ which will eventually be reintroduced in the final expression for the dielectric function. It is

$$\boldsymbol{\chi}_0^{-1}(\boldsymbol{q}_{\mathrm{mt}},\omega) = -\left[\begin{pmatrix} \mathbf{E}^{\mathrm{ip}}(\boldsymbol{q}_{\mathrm{mt}}) & 0 \\ 0 & \mathbf{E}^{\mathrm{ip}}(-\boldsymbol{q}_{\mathrm{mt}}) \end{pmatrix} - \omega\begin{pmatrix} \mathbb{1} & 0 \\ 0 & -\mathbb{1} \end{pmatrix}\right] \tag{3.20}$$

with the independent-particle transition energies as matrix elements (note that $\boldsymbol{k}_\pm$ implicit depends on $\boldsymbol{q}_{\mathrm{mt}}$)

$$E^{\mathrm{ip}}_{\alpha,\alpha'}(\boldsymbol{q}_{\mathrm{mt}}) = \left(\varepsilon_{u,\boldsymbol{k}_-} - \varepsilon_{o,\boldsymbol{k}_+}\right)\delta_{\alpha,\alpha'}. \tag{3.21}$$

Changing both k-summation variables from $\boldsymbol{k}$ to $-\boldsymbol{k}$ in the anti-resonant part of χ_0 and using the time-reversal symmetry (3.15) allows us to write

$$\sum_{o,u,\boldsymbol{k},\boldsymbol{k}'} \frac{\psi_{u,\boldsymbol{k}'}(\boldsymbol{r}_1)\psi^*_{o,\boldsymbol{k}}(\boldsymbol{r}'_1)\psi^*_{u,\boldsymbol{k}'}(\boldsymbol{r}'_2)\psi_{o,\boldsymbol{k}}(\boldsymbol{r}_2)}{-\omega-(\varepsilon_{u,\boldsymbol{k}'}-\varepsilon_{o,\boldsymbol{k}})+\mathrm{i}\delta} = \sum_{o,u,\boldsymbol{k},\boldsymbol{k}'} \frac{\psi^*_{u,\boldsymbol{k}'}(\boldsymbol{r}_1)\psi_{o,\boldsymbol{k}}(\boldsymbol{r}'_1)\psi_{u,\boldsymbol{k}'}(\boldsymbol{r}'_2)\psi^*_{o,\boldsymbol{k}}(\boldsymbol{r}_2)}{-\omega-(\varepsilon_{u,\boldsymbol{k}'}-\varepsilon_{o,\boldsymbol{k}})+\mathrm{i}\delta} \tag{3.22}$$

from which follows that $\boldsymbol{\chi}_0^{-1}$ can be written in the anti-resonant basis choice of eq. (3.16) as

$$\boldsymbol{\chi}_0^{-1}(\boldsymbol{q}_{\mathrm{mt}},\omega) = -\left[\begin{pmatrix}\mathbf{E}^{\mathrm{ip}}(\boldsymbol{q}_{\mathrm{mt}}) & 0\\ 0 & \mathbf{E}^{\mathrm{ip}}(\boldsymbol{q}_{\mathrm{mt}})\end{pmatrix} - \omega\begin{pmatrix}\mathbb{1} & 0\\ 0 & -\mathbb{1}\end{pmatrix}\right]. \tag{3.23}$$

Partial occupations

To account for partial occupation numbers of the Kohn-Sham system, we introduce the diagonal matrix of occupation number difference as

$$\mathbf{F}_{\alpha,\alpha'}(\boldsymbol{q}_{\mathrm{mt}}) = \left(f_{o,\boldsymbol{k}_+} - f_{u,\boldsymbol{k}_-}\right)\delta_{\alpha,\alpha'} \tag{3.24}$$

and rewrite eq. (3.23) in view of eq. (F.5) in a symmetric fashion (omitting $\boldsymbol{q}_{\mathrm{mt}}$)

$$\boldsymbol{\chi}_0^{-1}(\boldsymbol{q}_{\mathrm{mt}},\omega) = -\left[\begin{pmatrix}\mathbf{F}^{-\frac{1}{2}}\mathbf{E}^{\mathrm{ip}}\mathbf{F}^{-\frac{1}{2}} & 0\\ 0 & \mathbf{F}^{-\frac{1}{2}}\mathbf{E}^{\mathrm{ip}}\mathbf{F}^{-\frac{1}{2}}\end{pmatrix} - \omega\begin{pmatrix}\mathbb{1} & 0\\ 0 & -\mathbb{1}\end{pmatrix}\right]. \tag{3.25}$$

It is apparent, that this is an approximate approach and only possible as long as there is no occupation inversion.

3.3.2. Exchange interaction matrix elements

The calculation of the matrix elements of the Coulomb potential using eqs. (3.6) and (3.7) reduces to

$$V_{ij}(\boldsymbol{q}_{\mathrm{mt}}) = \iint \Upsilon^*_{i,\boldsymbol{q}_{\mathrm{mt}}}(\boldsymbol{r},\boldsymbol{r})v(\boldsymbol{r},\boldsymbol{r}')\Upsilon_{j,\boldsymbol{q}_{\mathrm{mt}}}(\boldsymbol{r}',\boldsymbol{r}')\,\mathrm{d}^3r\,\mathrm{d}^3r'\,. \tag{3.26}$$

The Coulomb potential is symmetrical in $\boldsymbol{r}$ and $\boldsymbol{r}'$ and obeys the lattice periodicity, i.e.

$$v(\boldsymbol{r},\boldsymbol{r}') = v(\boldsymbol{r}',\boldsymbol{r}) = v(|\boldsymbol{r}'-\boldsymbol{r}|) \quad \text{and} \quad v(\boldsymbol{r}+\boldsymbol{R},\boldsymbol{r}'+\boldsymbol{R}) = v(\boldsymbol{r},\boldsymbol{r}'). \tag{3.27}$$

Choosing the basis according to eq. (3.12), the elements of the four blocks are computed according to

$$\begin{aligned} V^{\mathrm{rr}}_{\alpha\alpha'}(\boldsymbol{q}_{\mathrm{mt}}) &= \left\langle o\boldsymbol{k}_+, u'\boldsymbol{k}'_- \middle| v(\boldsymbol{r},\boldsymbol{r}') \middle| u\boldsymbol{k}_-, o'\boldsymbol{k}'_+ \right\rangle \\ &\overset{(3.27)}{=} \left\langle u'\boldsymbol{k}'_-, o\boldsymbol{k}_+ \middle| v(\boldsymbol{r},\boldsymbol{r}') \middle| o'\boldsymbol{k}'_+, u\boldsymbol{k}_- \right\rangle \end{aligned} \tag{3.28a}$$

$$V^{\mathrm{aa}}_{\alpha\alpha'}(\boldsymbol{q}_{\mathrm{mt}}) = \left\langle u\boldsymbol{k}_+, o'\boldsymbol{k}'_- \middle| v(\boldsymbol{r},\boldsymbol{r}') \middle| o\boldsymbol{k}_-, u'\boldsymbol{k}'_+ \right\rangle \tag{3.28b}$$

$$V^{\mathrm{ra}}_{\alpha\alpha'}(\boldsymbol{q}_{\mathrm{mt}}) = \left\langle o\boldsymbol{k}_+, o'\boldsymbol{k}'_- \middle| v(\boldsymbol{r},\boldsymbol{r}') \middle| u\boldsymbol{k}_-, u'\boldsymbol{k}'_+ \right\rangle \tag{3.28c}$$

$$V^{\mathrm{ar}}_{\alpha\alpha'}(\boldsymbol{q}_{\mathrm{mt}}) = \left\langle u\boldsymbol{k}_+, u'\boldsymbol{k}'_- \middle| v(\boldsymbol{r},\boldsymbol{r}') \middle| o\boldsymbol{k}_-, o'\boldsymbol{k}'_+ \right\rangle . \tag{3.28d}$$

The rr-block elements correspond to the diagram 2.1.a, while the ra-block elements are depicted in the diagram 2.1.c. These four blocks become all equal when the basis functions of eq. (3.16) are used instead and the time-reversal symmetry is employed. This follows directly from eq. (3.16) and eq. (3.26). Consequently, only the resonant-resonant block of the exchange interaction matrix needs to be computed.

For further calculations, it is useful to use the lattice Fourier representation of the Coulomb potential v

$$v(\boldsymbol{r},\boldsymbol{r}') = \frac{1}{V}\sum_{\boldsymbol{G}}\sum_{\boldsymbol{q}\in\mathrm{B.z}} \frac{4\pi}{|\boldsymbol{G}+\boldsymbol{q}|}\mathrm{e}^{\mathrm{i}(\boldsymbol{G}+\boldsymbol{q})(\boldsymbol{r}-\boldsymbol{r}')} \tag{3.29}$$

and the plane-wave matrix elements M (see appendix D)

$$\left\langle f\boldsymbol{k}_f \middle| \mathrm{e}^{-\mathrm{i}(\boldsymbol{G}+\boldsymbol{q})\boldsymbol{r}} \middle| i\boldsymbol{k}_i \right\rangle = \delta_{\lfloor \boldsymbol{k}_f-\boldsymbol{k}_i+\boldsymbol{q}\rfloor_{1^{\mathrm{st}}\,\mathrm{BZ}},0}\, M_{fi\boldsymbol{k}_f}(\boldsymbol{G},\boldsymbol{q}), \tag{3.30}$$

where the Kronecker-delta ensures the conservation of crystal momentum. Then, the matrix elements (3.28a) take on the form

$$\begin{aligned} V^{\mathrm{rr}}_{\alpha\alpha'}(\boldsymbol{q}_{\mathrm{mt}}) = \frac{1}{V}\sum_{\boldsymbol{G}}\sum_{\boldsymbol{q}} v(\boldsymbol{G},\boldsymbol{q}) & \\ \times \left\langle u\boldsymbol{k}_- \middle| \mathrm{e}^{-\mathrm{i}(\boldsymbol{G}+\boldsymbol{q})\boldsymbol{r}} \middle| o\boldsymbol{k}_+ \right\rangle^* & \left\langle u'\boldsymbol{k}'_- \middle| \mathrm{e}^{-\mathrm{i}(\boldsymbol{G}+\boldsymbol{q})\boldsymbol{r}'} \middle| o'\boldsymbol{k}'_+ \right\rangle \\ &= \frac{1}{V}\sum_{\boldsymbol{G}} v(\boldsymbol{G},\boldsymbol{q}_{\mathrm{mt}}) M^*_{uo\boldsymbol{k}_-}(\boldsymbol{G},\boldsymbol{q}_{\mathrm{mt}}) M_{u'o'\boldsymbol{k}'_-}(\boldsymbol{G},\boldsymbol{q}_{\mathrm{mt}}). \end{aligned} \tag{3.31}$$

3.3.3. Screened Coulomb interaction

The matrix elements of the screened Coulomb interaction are computed with

$$W_{ij}(\boldsymbol{q}_{\mathrm{mt}}) = \iint \Upsilon^*_{i,\boldsymbol{q}_{\mathrm{mt}}}(\boldsymbol{r},\boldsymbol{r}') W(\boldsymbol{r},\boldsymbol{r}') \Upsilon_{j,\boldsymbol{q}_{\mathrm{mt}}}(\boldsymbol{r},\boldsymbol{r}')\, \mathrm{d}^3r\, \mathrm{d}^3r' , \tag{3.32}$$

where W is the statically screened Coulomb potential [see (2.16) and (2.28)]

$$W(\boldsymbol{r},\boldsymbol{r}') = \int v(\boldsymbol{r},\boldsymbol{r}'')\varepsilon^{-1}(\boldsymbol{r}'',\boldsymbol{r}')\, \mathrm{d}^3r'' . \tag{3.33}$$

For a crystalline system, we assume that W is real-valued and that

$$W(\boldsymbol{r},\boldsymbol{r}') = W(\boldsymbol{r}',\boldsymbol{r}) \quad \text{and} \quad W(\boldsymbol{r}+\boldsymbol{R},\boldsymbol{r}'+\boldsymbol{R}) = W(\boldsymbol{r},\boldsymbol{r}') \tag{3.34}$$

hold. Then, in the basis (3.12), the four blocks are given by

$$\begin{aligned} W^{\mathrm{rr}}_{\alpha\alpha'}(\boldsymbol{q}_{\mathrm{mt}}) &= \left\langle o\boldsymbol{k}_+, u'\boldsymbol{k}'_- \middle| W(\boldsymbol{r},\boldsymbol{r}') \middle| o'\boldsymbol{k}'_+, u\boldsymbol{k}_- \right\rangle \\ &\overset{(3.34)}{=} \left\langle u'\boldsymbol{k}'_-, o\boldsymbol{k}_+ \middle| W(\boldsymbol{r},\boldsymbol{r}') \middle| u\boldsymbol{k}_-, o'\boldsymbol{k}'_+ \right\rangle \end{aligned} \tag{3.35a}$$

$$W^{\mathrm{aa}}_{\alpha\alpha'}(\boldsymbol{q}_{\mathrm{mt}}) = \left\langle u\boldsymbol{k}_{+}, o'\boldsymbol{k}'_{-} \middle| W(\boldsymbol{r},\boldsymbol{r}') \middle| u'\boldsymbol{k}'_{+}, o\boldsymbol{k}_{-} \right\rangle \tag{3.35b}$$

$$W^{\mathrm{ra}}_{\alpha\alpha'}(\boldsymbol{q}_{\mathrm{mt}}) = \left\langle o\boldsymbol{k}_{+}, o'\boldsymbol{k}'_{-} \middle| W(\boldsymbol{r},\boldsymbol{r}') \middle| u'\boldsymbol{k}'_{+}, u\boldsymbol{k}_{-} \right\rangle \tag{3.35c}$$

$$W^{\mathrm{ar}}_{\alpha\alpha'}(\boldsymbol{q}_{\mathrm{mt}}) = \left\langle u\boldsymbol{k}_{+}, u'\boldsymbol{k}'_{-} \middle| W(\boldsymbol{r},\boldsymbol{r}') \middle| o'\boldsymbol{k}'_{+}, o\boldsymbol{k}_{-} \right\rangle . \tag{3.35d}$$

For the case of zero-momentum transfer, $\boldsymbol{q}_{\mathrm{mt}} = 0$, these blocks are related according to

$$\mathsf{W}^{\mathrm{rr}} = \left(\mathsf{W}^{\mathrm{rr}}\right)^{\dagger} = \left(\mathsf{W}^{\mathrm{aa}}\right)^{*} \quad \text{and} \quad \mathsf{W}^{\mathrm{ra}} = \left(\mathsf{W}^{\mathrm{ra}}\right)^{\mathrm{T}} = \left(\mathsf{W}^{\mathrm{ar}}\right)^{*} . \tag{3.36}$$

For finite momentum transfer these relations do not hold anymore and four distinct blocks are left.

Again, this can be remedied by switching to the basis defined in eq. (3.16) and using the time-reversal symmetry. From eqs. (3.16), (3.32) and (3.34) it follows directly that there are only two distinct blocks, because

$$\mathsf{W}^{\mathrm{rr}} = \mathsf{W}^{\bar{\mathrm{a}}\bar{\mathrm{a}}} = \left(\mathsf{W}^{\mathrm{rr}}\right)^{\dagger} \quad \text{and} \quad \mathsf{W}^{\mathrm{r}\bar{\mathrm{a}}} = \mathsf{W}^{\bar{\mathrm{a}}\mathrm{r}} = \left(\mathsf{W}^{\mathrm{r}\bar{\mathrm{a}}}\right)^{\dagger} . \tag{3.37}$$

This result also holds for finite momentum transfer. In terms of the single particle states the elements of $\mathsf{W}^{\mathrm{r}\bar{\mathrm{a}}}$ are calculated according to

$$\begin{aligned}
W^{\mathrm{r}\bar{\mathrm{a}}}_{\alpha\alpha'}(\boldsymbol{q}_{\mathrm{mt}}) &= \iint \Upsilon^{\mathrm{r}*}_{\alpha}(\boldsymbol{r},\boldsymbol{r}') W(\boldsymbol{r},\boldsymbol{r}') \Upsilon^{\mathrm{r}}_{\alpha'}(\boldsymbol{r}',\boldsymbol{r}) \\
&= \iint \phi^{*}_{o\boldsymbol{k}_{+}}(\boldsymbol{r}) \phi_{u\boldsymbol{k}_{-}}(\boldsymbol{r}') W(\boldsymbol{r},\boldsymbol{r}') \phi_{o'\boldsymbol{k}'_{+}}(\boldsymbol{r}') \phi^{*}_{u'\boldsymbol{k}_{-}}(\boldsymbol{r}) \, \mathrm{d}^3 r \, \mathrm{d}^3 r' \\
&= \iint \phi^{*}_{o\boldsymbol{k}_{+}}(\boldsymbol{r}) \phi_{o'\boldsymbol{k}'_{+}}(\boldsymbol{r}') W(\boldsymbol{r},\boldsymbol{r}') \phi^{*}_{u'\boldsymbol{k}_{-}}(\boldsymbol{r}) \phi_{u\boldsymbol{k}_{-}}(\boldsymbol{r}') \, \mathrm{d}^3 r \, \mathrm{d}^3 r' \\
&:= \left\langle o\boldsymbol{k}_{+}, (o'\boldsymbol{k}'_{+})^{*} \middle| W(\boldsymbol{r},\boldsymbol{r}') \middle| (u'\boldsymbol{k}'_{-})^{*}, u\boldsymbol{k}_{-} \right\rangle \\
&\overset{(3.34)}{=} \left\langle (o'\boldsymbol{k}'_{+})^{*}, o\boldsymbol{k}_{+} \middle| W(\boldsymbol{r},\boldsymbol{r}') \middle| u\boldsymbol{k}_{-}, (u'\boldsymbol{k}'_{-})^{*} \right\rangle .
\end{aligned} \tag{3.38}$$

As for the exchange interaction, we use the lattice Fourier representation of $W(\boldsymbol{r},\boldsymbol{r}')$. Plugging into eq. (3.33) the Fourier representations of the Coulomb potential and of the inverse dielectric function and integrating over the doubly-primed coordinates yields

$$W(\boldsymbol{r},\boldsymbol{r}') = \frac{1}{V} \sum_{\boldsymbol{G}\boldsymbol{G}'} \sum_{\boldsymbol{q}\in\mathrm{B.z}} \mathrm{e}^{\mathrm{i}(\boldsymbol{G}+\boldsymbol{q})\boldsymbol{r}} W_{\boldsymbol{G},\boldsymbol{G}'}(\boldsymbol{q}) \, \mathrm{e}^{-\mathrm{i}(\boldsymbol{G}'+\boldsymbol{q})\boldsymbol{r}'} , \tag{3.39}$$

with the coefficients

$$W_{\boldsymbol{G},\boldsymbol{G}'}(\boldsymbol{q}) = \frac{4\pi}{|\boldsymbol{G}+\boldsymbol{q}|^2} \varepsilon^{-1}_{\boldsymbol{G}\boldsymbol{G}'}(\boldsymbol{q}, \omega = 0). \tag{3.40}$$

The appearance of ε, which is our target quantity, in the setup of the screened interaction signals that, in theory, the BSE needs to be solved self-consistently starting from some approximation to ε. In practice, however, the microscopic dielectric matrix in the independent particle approximation $\varepsilon^0_{\boldsymbol{G}\boldsymbol{G}'}(\boldsymbol{q}, \omega = 0)$ is used for a one-shot BSE calculation. For the construction of ε^0 the retarded polarizability (see section 1.2) P is calculated for the Kohn-Sham system and the exchange-correlation kernel is neglected (see appendix E).

The resonant-resonant-block of W eq. (3.35a) can then be stated in terms of the plane-wave matrix elements (3.30) as

$$\begin{aligned} W^{\mathrm{rr}}_{\alpha\alpha'}(\boldsymbol{q}_{\mathrm{mt}}) &= \frac{1}{V}\sum_{\boldsymbol{G}\boldsymbol{G}'}\sum_{\boldsymbol{q}} W_{\boldsymbol{G}\boldsymbol{G}'}(\boldsymbol{q}) \left\langle o'\boldsymbol{k}'_+ \middle| \mathrm{e}^{-\mathrm{i}(\boldsymbol{G}+\boldsymbol{q})\boldsymbol{r}} \middle| o\boldsymbol{k}_+ \right\rangle^* \left\langle u'\boldsymbol{k}'_- \middle| \mathrm{e}^{-\mathrm{i}(\boldsymbol{G}'+\boldsymbol{q})\boldsymbol{r}'} \middle| u\boldsymbol{k}_- \right\rangle \\ &= \frac{1}{V}\sum_{\boldsymbol{G}\boldsymbol{G}'} W_{\boldsymbol{G}\boldsymbol{G}'}(\boldsymbol{k}-\boldsymbol{k}') M^*_{o'o\boldsymbol{k}'_+}(\boldsymbol{G}, \boldsymbol{k}-\boldsymbol{k}') M_{u'u\boldsymbol{k}'_-}(\boldsymbol{G}', \boldsymbol{k}-\boldsymbol{k}') \\ &\overset{(3.34)}{=} \frac{1}{V}\sum_{\boldsymbol{G}\boldsymbol{G}'} W_{\boldsymbol{G}\boldsymbol{G}'}(\boldsymbol{k}'-\boldsymbol{k}) M^*_{uu'\boldsymbol{k}_-}(\boldsymbol{G}, \boldsymbol{k}'-\boldsymbol{k}) M_{oo'\boldsymbol{k}_+}(\boldsymbol{G}', \boldsymbol{k}'-\boldsymbol{k}), \end{aligned} \tag{3.41}$$

while the coupling block eq. (3.38) takes on the form of

$$\begin{aligned} W^{\mathrm{r\bar{a}}}_{\alpha\alpha'}(\boldsymbol{q}_{\mathrm{mt}}) &= \frac{1}{V}\sum_{\boldsymbol{G}\boldsymbol{G}'}\sum_{\boldsymbol{q}} W_{\boldsymbol{G}\boldsymbol{G}'}(\boldsymbol{q}) \left\langle u\boldsymbol{k}_- \middle| \mathrm{e}^{-\mathrm{i}(\boldsymbol{G}+\boldsymbol{q})\boldsymbol{r}} \middle| (o'\boldsymbol{k}'_+)^* \right\rangle^* \left\langle o\boldsymbol{k}_+ \middle| \mathrm{e}^{-\mathrm{i}(\boldsymbol{G}'+\boldsymbol{q})\boldsymbol{r}'} \middle| (u'\boldsymbol{k}'_-)^* \right\rangle \\ &= \frac{1}{V}\sum_{\boldsymbol{G}\boldsymbol{G}'} W_{\boldsymbol{G}\boldsymbol{G}'}(-\boldsymbol{k}'-\boldsymbol{k}) N^*_{uo'\boldsymbol{k}_-}(\boldsymbol{G}, -\boldsymbol{k}'-\boldsymbol{k}) N_{ou'\boldsymbol{k}_+}(\boldsymbol{G}', -\boldsymbol{k}'-\boldsymbol{k}), \end{aligned} \tag{3.42}$$

where we used the symmetry again and introduced the modified plane wave matrix elements N

$$\left\langle f\boldsymbol{k}_f \middle| \mathrm{e}^{-\mathrm{i}(\boldsymbol{G}+\boldsymbol{q})\boldsymbol{r}} \middle| (i\boldsymbol{k}_i)^* \right\rangle =: \delta_{\lfloor \boldsymbol{k}_f+\boldsymbol{k}_i+\boldsymbol{q} \rfloor_{1^{\mathrm{st}}\,\mathrm{BZ}},0}\, N_{fi\boldsymbol{k}_f}(\boldsymbol{G}, \boldsymbol{q}). \tag{3.43}$$

They are related to the plane-wave matix elments M due to the time-reversal symmetry

$$\left\langle f\boldsymbol{k}_f \middle| \mathrm{e}^{-\mathrm{i}(\boldsymbol{G}+\boldsymbol{q})\boldsymbol{r}} \middle| (i\boldsymbol{k}_i)^* \right\rangle = \left\langle f\boldsymbol{k}_f \middle| \mathrm{e}^{-\mathrm{i}(\boldsymbol{G}+\boldsymbol{q})\boldsymbol{r}} \middle| i-\boldsymbol{k}_i \right\rangle. \tag{3.44}$$

The advantage of calculating the Ns directly, is that we do not need to calculated the $\left|-\boldsymbol{k}_i\right\rangle$ eigenstates and that we fix the phase between $|-\boldsymbol{k}\rangle$ and $(|\boldsymbol{k}\rangle)^*$ implicitly to 1.

3.4. BSE as an eigenvalue problem

With the results of 3.3 we can write eq. (3.13) as

$$\boldsymbol{\chi}(\boldsymbol{q}_{\mathrm{mt}}, \omega) = -\mathbf{F}^{\frac{1}{2}}(\boldsymbol{q}_{\mathrm{mt}}) \left[\mathbf{H}^{\mathrm{e}}(\boldsymbol{q}_{\mathrm{mt}}) - \omega\boldsymbol{\Delta}\right]^{-1} \mathbf{F}^{\frac{1}{2}}(\boldsymbol{q}_{\mathrm{mt}}), \tag{3.45}$$

where we introduce the effective two-particle Hamiltonian $\mathbf{H}^{\mathrm{e}}$,

$$\boldsymbol{\Delta} = \begin{pmatrix} \mathbb{1} & 0 \\ 0 & -\mathbb{1} \end{pmatrix} \quad \text{and redefine} \quad \mathbf{F}^{\frac{1}{2}} = \begin{pmatrix} \mathbf{F}^{\frac{1}{2}} & 0 \\ 0 & \mathbf{F}^{\frac{1}{2}} \end{pmatrix}. \tag{3.46}$$

Using time-reversal symmetry as discussed above, the Hamiltonian is hermitian and takes on the form

$$\mathbf{H}^{\mathrm{e}}(\boldsymbol{q}_{\mathrm{mt}}) = \mathbf{F}^{\frac{1}{2}}(\boldsymbol{q}_{\mathrm{mt}}) \begin{pmatrix} \mathbf{A}(\boldsymbol{q}_{\mathrm{mt}}) & \mathbf{B}(\boldsymbol{q}_{\mathrm{mt}}) \\ \mathbf{B}(\boldsymbol{q}_{\mathrm{mt}}) & \mathbf{A}(\boldsymbol{q}_{\mathrm{mt}}) \end{pmatrix} \mathbf{F}^{\frac{1}{2}}(\boldsymbol{q}_{\mathrm{mt}}). \tag{3.47}$$

The diagonal block is given by

$$\mathbf{A}(\boldsymbol{q}_{\mathrm{mt}}) = \mathbf{E}^{\mathrm{ip}}(\boldsymbol{q}_{\mathrm{mt}}) + 2\gamma_{\mathrm{x}} \mathbf{V}^{\mathrm{rr}}(\boldsymbol{q}_{\mathrm{mt}}) - \gamma_{\mathrm{c}} \mathbf{W}^{\mathrm{rr}}(\boldsymbol{q}_{\mathrm{mt}}), \tag{3.48}$$

and the coupling block by

$$\mathbf{B}(\boldsymbol{q}_{\mathrm{mt}}) = 2\gamma_{\mathrm{x}} \mathbf{V}^{\mathrm{rr}}(\boldsymbol{q}_{\mathrm{mt}}) - \gamma_{\mathrm{c}} \mathbf{W}^{\mathrm{r\bar{a}}}(\boldsymbol{q}_{\mathrm{mt}}). \tag{3.49}$$

Here, we introduce the factors γ_x and γ_{c} which allow to account for the spin degree of freedom, as discussed in Ref. [10]. Spin-singlet excitations are obtained by setting $\gamma_{\mathrm{x}} = 1$ and $\gamma_{\mathrm{c}} = 1$, and spin-triplet excitations are calculated with $\gamma_{\mathrm{x}} = 0$ and $\gamma_{\mathrm{c}} = 1$. This treatment is allowed as long as the spin-up and spin-down components of the orbitals are considered to be identical.

The resolvent (3.45) can be found using the solutions of the generalized eigenvalue problem (dropping the $\boldsymbol{q}_{\mathrm{mt}}$ for brevity)

$$\mathbf{H}^{\mathrm{e}} \begin{pmatrix} \boldsymbol{X}_\lambda \\ \boldsymbol{Y}_\lambda \end{pmatrix} = E_\lambda \boldsymbol{\Delta} \begin{pmatrix} \boldsymbol{X}_\lambda \\ \boldsymbol{Y}_\lambda \end{pmatrix}, \tag{3.50}$$

according to [27]

$$\left[\mathbf{H}^{\mathrm{e}} - \omega \boldsymbol{\Delta}\right]^{-1} = \sum_\lambda \left[\frac{1}{E_\lambda - \omega} \begin{pmatrix} \boldsymbol{X}_\lambda \\ \boldsymbol{Y}_\lambda \end{pmatrix} \begin{pmatrix} \boldsymbol{X}_\lambda \\ \boldsymbol{Y}_\lambda \end{pmatrix}^\dagger + \frac{1}{E_\lambda + \omega} \begin{pmatrix} \boldsymbol{Y}_\lambda \\ \boldsymbol{X}_\lambda \end{pmatrix} \begin{pmatrix} \boldsymbol{Y}_\lambda \\ \boldsymbol{X}_\lambda \end{pmatrix}^\dagger \right]. \tag{3.51}$$

3.4.1. Squared eigenvalue problem

The generalized eigenvalue problem eq. (3.50) can be mapped, following [26, 27], onto an auxiliary “squared” EVP of half its size, given by

$$\mathbf{S} = (\mathbf{A} - \mathbf{B})^{\frac{1}{2}} (\mathbf{A} + \mathbf{B}) (\mathbf{A} - \mathbf{B})^{\frac{1}{2}} \tag{3.52a}$$

and

$$\mathbf{S} \boldsymbol{Z}_\lambda = W_\lambda \boldsymbol{Z}_\lambda. \tag{3.52b}$$

As long as $\mathbf{A} - \mathbf{B}$ and $\mathbf{A} + \mathbf{B}$ are positive definite, the solutions of eq. (3.50) are exactly given by

$$E_\lambda = \sqrt{W_\lambda}, \tag{3.53a}$$

$$\left(\boldsymbol{X}_\lambda + \boldsymbol{Y}_\lambda\right) = (\mathbf{A} - \mathbf{B})^{\frac{1}{2}} \frac{1}{\sqrt{E_\lambda}} \boldsymbol{Z}_\lambda, \tag{3.53b}$$

and

$$\left(\boldsymbol{X}_\lambda - \boldsymbol{Y}_\lambda\right) = (\mathbf{A} - \mathbf{B})^{\frac{1}{2}} \sqrt{E_\lambda} \boldsymbol{Z}_\lambda. \tag{3.53c}$$

Using the shorthand notation

$$\mathsf{C} = (\mathsf{A} - \mathsf{B})^{\frac{1}{2}} \tag{3.54}$$

and the scaling factors

$$E_\lambda^\pm = \frac{1}{\sqrt{E_\lambda}} \pm \sqrt{E_\lambda}, \tag{3.55}$$

we can write

$$\begin{pmatrix} \boldsymbol{X}_\lambda \\ \boldsymbol{Y}_\lambda \end{pmatrix} = \frac{1}{2} \begin{pmatrix} \mathsf{C} E_\lambda^+ \boldsymbol{Z}_\lambda \\ \mathsf{C} E_\lambda^- \boldsymbol{Z}_\lambda \end{pmatrix}. \tag{3.56}$$

3.5. Density correlation function

The time-ordered density correlation function $\chi(\boldsymbol{r}, \boldsymbol{r}', \omega)$ can now be calculated using the matrix elements χ_{ij} and the basis functions according to

$$\chi(\boldsymbol{r}, \boldsymbol{r}', \omega) = \chi(\boldsymbol{r}, \boldsymbol{r}', \boldsymbol{r}, \boldsymbol{r}', \omega) = \sum_{ij} \Upsilon_i(\boldsymbol{r}, \boldsymbol{r}) \chi_{ij}(\omega) \Upsilon_j^*(\boldsymbol{r}', \boldsymbol{r}'). \tag{3.57}$$

A subsequent Fourier transform yields the form (1.37)

$$\begin{aligned} \chi_{\boldsymbol{G}\boldsymbol{G}'}(\boldsymbol{q}_\mathrm{mt}, \omega) &= \frac{1}{V} \iint \mathrm{e}^{-\mathrm{i}(\boldsymbol{G}+\boldsymbol{q}_\mathrm{mt})\boldsymbol{r}} \chi(\boldsymbol{r}, \boldsymbol{r}', \omega) \mathrm{e}^{\mathrm{i}(\boldsymbol{G}'+\boldsymbol{q}_\mathrm{mt})\boldsymbol{r}'} \, \mathrm{d}^3\boldsymbol{r} \, \mathrm{d}^3\boldsymbol{r}' \\ &= \frac{1}{V} \sum_{ij} \left(\int \Upsilon_i(\boldsymbol{r}, \boldsymbol{r}) \mathrm{e}^{-\mathrm{i}(\boldsymbol{G}+\boldsymbol{q}_\mathrm{mt})\boldsymbol{r}} \mathrm{d}^3\boldsymbol{r} \right) \chi_{ij}(\omega) \left(\int \Upsilon_j(\boldsymbol{r}', \boldsymbol{r}') \mathrm{e}^{-\mathrm{i}(\boldsymbol{G}'+\boldsymbol{q}_\mathrm{mt})\boldsymbol{r}'} \, \mathrm{d}^3\boldsymbol{r}' \right)^* \\ &= \frac{1}{V} \sum_{ij} M_i(\boldsymbol{G}, \boldsymbol{q}_\mathrm{mt}) \chi_{ij}(\omega) M_j^*(\boldsymbol{G}', \boldsymbol{q}_\mathrm{mt}). \end{aligned} \tag{3.58}$$

Here, the plane-wave matrix elements M ensure that only basis functions with the Bloch periodicity $\boldsymbol{q}_\mathrm{mt}$ are needed. For the resonant basis functions, the associated plane-wave elements are

$$M_\alpha^\mathrm{r}(\boldsymbol{G}, \boldsymbol{q}_\mathrm{mt}) = \int \Upsilon_{\alpha,\boldsymbol{q}}^\mathrm{r}(\boldsymbol{r}, \boldsymbol{r}) \mathrm{e}^{-\mathrm{i}(\boldsymbol{G}+\boldsymbol{q}_\mathrm{mt})\boldsymbol{r}} \, \mathrm{d}^3 r = \delta_{\boldsymbol{q}_\mathrm{mt},\boldsymbol{q}} M_{uo\boldsymbol{k}\_}(\boldsymbol{G}, \boldsymbol{q}_\mathrm{mt}) \tag{3.59}$$

that are equal to the anti-resonant ones when the time-reversal symmetry is used. In view of eq. (3.45) we also absorb the occupation factors into the projecting plane wave elements

$$\tilde{\boldsymbol{M}}(\boldsymbol{G}, \boldsymbol{q}_\mathrm{mt}) = \mathsf{F}^{\frac{1}{2}} \boldsymbol{M}^\mathrm{r}(\boldsymbol{G}, \boldsymbol{q}_\mathrm{mt}) \tag{3.60}$$

so that

$$\chi_{\boldsymbol{G}\boldsymbol{G}'}(\boldsymbol{q}_\mathrm{mt}, \omega) = -\frac{1}{V} \sum_{ij} \tilde{M}_i(\boldsymbol{G}, \boldsymbol{q}_\mathrm{mt}) \left[\mathsf{H}^\mathrm{e} - \omega \boldsymbol{\Delta}\right]_{ij}^{-1} \tilde{M}_j^*(\boldsymbol{G}', \boldsymbol{q}_\mathrm{mt}). \tag{3.61}$$

Combining the expressions of eq. (3.58) and of the matrix $\boldsymbol{\chi}$ in terms of the eigenvectors (3.51) yields

$$\chi_{\boldsymbol{G}\boldsymbol{G}'}^\mathrm{T}(\boldsymbol{q}_\mathrm{mt}, \omega) = \sum_\lambda \left(\frac{1}{\omega - E_\lambda + \mathrm{i}\delta} + \frac{1}{-\omega - E_\lambda + \mathrm{i}\delta} \right) t_\lambda^*(\boldsymbol{G}, \boldsymbol{q}_\mathrm{mt}) t_\lambda(\boldsymbol{G}', \boldsymbol{q}_\mathrm{mt}), \tag{3.62}$$

where we have introduced the *transition coefficients* t_λ

$$t_\lambda(\boldsymbol{G}, \boldsymbol{q}_{\mathrm{mt}}) = \left(\boldsymbol{X}_\lambda + \boldsymbol{Y}_\lambda\right)^\dagger \tilde{\boldsymbol{M}}^{\mathrm{r}*}(\boldsymbol{G}, \boldsymbol{q}_{\mathrm{mt}}) = \left[\mathsf{C}\frac{1}{\sqrt{E_\lambda}}\boldsymbol{Z}_\lambda\right]^\dagger \tilde{\boldsymbol{M}}^{\mathrm{r}*}(\boldsymbol{G}, \boldsymbol{q}_{\mathrm{mt}}). \tag{3.63}$$

They constitute a sum of weighted plane wave transition matrix elements, where the weights are given by the corresponding BSE eigenvectors. In order to go over to the retarded density correlation function we need to replace iδ by $-$iδ in the second denominator of eq. (3.62) [16], leading to

$$\chi^{\mathrm{R}}_{\boldsymbol{G}\boldsymbol{G}'}(\boldsymbol{q}_{\mathrm{mt}}, \omega) = \sum_\lambda \left(\frac{1}{\omega - E_\lambda + \mathrm{i}\delta} + \frac{1}{-\omega - E_\lambda - \mathrm{i}\delta}\right) t^*_\lambda(\boldsymbol{G}, \boldsymbol{q}_{\mathrm{mt}}) t_\lambda(\boldsymbol{G}', \boldsymbol{q}_{\mathrm{mt}}). \tag{3.64}$$

Thus, the macroscopic dielectric function defined in eq. (1.41) can be expressed in terms of χ^{R} using eq. (1.37) as

$$\varepsilon_{\mathrm{M}}(\boldsymbol{Q}_{\mathrm{mt}}, \omega) = \left[1 + v_{\boldsymbol{G}_{\mathrm{mt}}}(\boldsymbol{q}_{\mathrm{mt}}) \sum_\lambda \left(\frac{1}{\omega - E_\lambda + \mathrm{i}\delta} + \frac{1}{-\omega - E_\lambda - \mathrm{i}\delta}\right) \left|t_\lambda(\boldsymbol{G}_{\mathrm{mt}}, \boldsymbol{q}_{\mathrm{mt}})\right|^2\right]^{-1}. \tag{3.65}$$

The square moduli of the transition coefficients t_λ are also referred to as *the oscillator strengths*.

3.6. The Tamm-Dancoff approximation

As already discussed in 2.3.5, a common approximation to the BSE is to zero the coupling block between the resonant and anti-resonant subspace eq. (3.47). Doing so, one is left with two decoupled eigenvalue problems for the resonant and the anti-resonant subspace, which are identical when the time-reversal symmetry is used. In this case, only the solutions of

$$\mathsf{H}^{\mathrm{e,\,TDA}} = \mathsf{F}^{\frac{1}{2}}\mathsf{A}(\boldsymbol{q}_{\mathrm{mt}})\mathsf{F}^{\frac{1}{2}}\boldsymbol{X}_\lambda = E_\lambda \boldsymbol{X}_\lambda \tag{3.66}$$

enter the expression for the transition coefficients t_λ (3.63),

$$t^{\mathrm{TDA}}_\lambda(\boldsymbol{G}_{\mathrm{mt}}, \boldsymbol{q}_{\mathrm{mt}}) = \boldsymbol{X}^\dagger_\lambda \tilde{\boldsymbol{M}}^{\mathrm{r}*}(\boldsymbol{G}_{\mathrm{mt}}, \boldsymbol{q}_{\mathrm{mt}}). \tag{3.67}$$

In [26] it is warned against the use of eq. (3.65) with the TDA, and it is suggested to use the extension of the scheme discussed in section 1.5.1 to finite momentum transfer. This is done by setting the corresponding $\boldsymbol{G}_{\mathrm{mt}}$ component of of the bare Coulomb potential to zero in the BSE setup and calculate the dielectric function according to

$$\varepsilon^{\mathrm{TDA}}_{\mathrm{M}}(\boldsymbol{Q}_{\mathrm{mt}}, \omega) = 1 - v_{\boldsymbol{G}_{\mathrm{mt}}}(\boldsymbol{q}_{\mathrm{mt}}) \sum_\lambda \left(\frac{1}{\omega - E_\lambda + \mathrm{i}\delta} + \frac{1}{-\omega - E_\lambda - \mathrm{i}\delta}\right) \left|t^{\mathrm{TDA}}_\lambda(\boldsymbol{G}_{\mathrm{mt}}, \boldsymbol{q}_{\mathrm{mt}})\right|^2. \tag{3.68}$$

In the calculations of the current work it was confirmed, that this procedure indeed yields significantly more accurate results when the TDA results are compared to the non-TDA calculations and experimental data.

3.7. Optical limit

For excitations with light in the optical range, i.e. 400 nm – 700 nm, the momentum transfer to the electron is negligible. For example, a photon with a wave-length of 400 nm carries a momentum of $\sim 1 \times 10^{-3}$ in atomic units. Thus, we will investigate the limit of $\boldsymbol{q} \to 0$ in the following. As discussed in section 1.5.1, to treat this limit it is useful to compute the modified polarizability $\bar{P}$ instead of the susceptibility χ. In the context of the BSE, this just amounts to replace the full Coulomb potential in the exchange term, eq. (3.26), with the long-range-truncated one eq. (1.44) [8]. Equation (3.64) then becomes

$$\bar{P}^{\mathrm{R}}_{\boldsymbol{G}\boldsymbol{G}'}(\boldsymbol{q}_{\mathrm{mt}}, \omega) = \sum_{\lambda} \left(\frac{1}{\omega - E_\lambda + \mathrm{i}\delta} + \frac{1}{-\omega - E_\lambda - \mathrm{i}\delta} \right) t^*_\lambda(\boldsymbol{G}, \boldsymbol{q}_{\mathrm{mt}}) t_\lambda(\boldsymbol{G}', \boldsymbol{q}_{\mathrm{mt}}). \tag{3.69}$$

In order to take the limit $\boldsymbol{G} = 0$, $\boldsymbol{G}' = 0$, and $\boldsymbol{q}_{\mathrm{mt}} \to 0$, we first approximate the plane-wave matrix elements by the dipole matrix elements D (see D.2)

$$M^{\mathrm{r}}_{\alpha}(0, \boldsymbol{q}) \overset{q \ll 1}{=} \mathrm{i} \sum_{j} D^{\mathrm{r}}_{\alpha,j} q_j, \tag{3.70}$$

where we define the resonant dipole matrix elements in terms of the momentum operator as

$$D^{\mathrm{r}}_{\alpha,j} = \mathrm{i} \frac{\langle u\boldsymbol{k} | \hat{p}_j | o\boldsymbol{k} \rangle}{\epsilon_{u\boldsymbol{k}} - \epsilon_{o\boldsymbol{k}}}. \tag{3.71}$$

Inserting eq. (3.70) into eq. (3.63) yields for the transition coefficients

$$t_\lambda(0, \boldsymbol{q}) = -\mathrm{i} \left(\boldsymbol{X}_\lambda + \boldsymbol{Y}_\lambda \right)^\dagger \mathsf{F}^{\frac{1}{2}} \mathsf{D}^{\mathrm{r}*} \frac{\hat{\boldsymbol{q}}}{|\boldsymbol{q}|} =: -\mathrm{i} \left(\boldsymbol{X}_\lambda + \boldsymbol{Y}_\lambda \right)^\dagger \tilde{\mathsf{D}}^{\mathrm{r}*} \frac{\hat{\boldsymbol{q}}}{|\boldsymbol{q}|}. \tag{3.72}$$

where $\hat{\boldsymbol{q}}$ is the unit vector along the direction of $\boldsymbol{q}$, and we have included the occupation factors into D. This allows us to cancel the $1/|\boldsymbol{q}|^2$ factor of the Coulomb potential, and we write

$$\begin{aligned} \varepsilon_{\mathrm{M}}(\omega) &= 1 - \lim_{q \to 0} \frac{4\pi}{q^2} \bar{P}_{0,0}(\boldsymbol{q}, \omega) \\ &= 1 - 4\pi \sum_{i,j} \hat{q}_i \left(\sum_{\lambda} \left(\frac{1}{\omega - E_\lambda + \mathrm{i}\delta} + \frac{1}{-\omega - E_\lambda - \mathrm{i}\delta} \right) t^*_{\lambda,i} t_{\lambda,j} \right) \hat{q}_j, \end{aligned} \tag{3.73}$$

where

$$t_{\lambda,i} = -\mathrm{i} \sum_{\alpha} \left(\boldsymbol{X}_\lambda + \boldsymbol{Y}_\lambda \right)^\dagger_\alpha \tilde{\mathsf{D}}^{\mathrm{r}*}_{\alpha,i} \tag{3.74}$$

define the transition coefficients for each Cartesian direction. From this expression we can recover the form of the (macroscopic) transversal dielectric matrix eq. (1.30)

$$\varepsilon^{ij}_{\mathrm{M}}(\omega) = \delta_{ij} - 4\pi \sum_{\lambda} \left(\frac{1}{\omega - E_\lambda + \mathrm{i}\delta} + \frac{1}{-\omega - E_\lambda - \mathrm{i}\delta} \right) t^*_{\lambda,i} t_{\lambda,j}. \tag{3.75}$$

As noted in section 1.4, we are mainly interested in the imaginary part of ε which is given by a sum of scaled positive and negative Lorentzian functions of width δ centered at the positive and negative BSE eigen-energies, respectively. The roots of the real part, on the other hand, are also useful to interpret the spectrum in terms of the classical Drude-Lorentz model. They can be used to determine the positions of plasmoic excitations [28].

$$\mathfrak{I}\left[\varepsilon_{\mathrm{M}}^{ii}(\omega)\right] = \sum_{\lambda} 4\pi^2 \left|t_{\lambda,i}\right|^2 \left(\frac{1}{\pi\delta} \frac{\delta^2}{(\omega - E_\lambda)^2 + \delta^2} - \frac{1}{\pi\delta} \frac{\delta^2}{(\omega + E_\lambda)^2 + \delta^2} \right), \tag{3.76a}$$

$$\mathfrak{R}\left[\varepsilon_{\mathrm{M}}^{ii}(\omega)\right] = 1 - \sum_{\lambda} 4\pi^2 \left|t_{\lambda,i}\right|^2 \left(\frac{1}{\pi} \frac{\omega - E_\lambda}{(\omega - E_\lambda)^2 + \delta^2} - \frac{1}{\pi} \frac{\omega + E_\lambda}{(\omega + E_\lambda)^2 + \delta^2} \right). \tag{3.76b}$$

The scaling factors are determined by the oscillator strengths.

A. Bloch states

This appendix summarizes the well-known results of Bloch's theory of electrons in a periodic potential in appendices A.1 to A.3. In particular, the effect of the time reversal symmetry of the underlying Hamiltonian is discussed in appendix A.3.2.

A.1. Crystal lattices

We consider a solid as an infinite periodic assembly of ions. The crystalline structure is defined by the *real space lattice vectors* $\{\boldsymbol{R}\}$ that are spanned by all integer combinations of the corresponding *real space basis vectors* $\left\{\boldsymbol{a}_i\right\}$. The volume spanned by the basis vectors is the volume of the *unit cell* denoted as Ω. An associated *basis in reciprocal space* $\left\{\boldsymbol{b}_i\right\}$ is defined by

$$\boldsymbol{a}_i \cdot \boldsymbol{b}_j = 2\pi\delta_{i,j}. \tag{A.1}$$

Integer combinations of the reciprocal basis vectors define the *reciprocal lattice vectors* $\{\boldsymbol{G}\}$. Any point in reciprocal space can then be expressed as $\boldsymbol{k} = \boldsymbol{q} + \boldsymbol{G}$, where $\boldsymbol{q}$ is a vector within the *reciprocal unit cell.*

A.2. Electron in a perfect crystal

The common way to approach the quantum-mechanical description of a solid is to first consider one electron in a potential which is periodic with respect to translations along the lattice vectors $\{\boldsymbol{R}\}$

$$U(\boldsymbol{r} + \boldsymbol{R}) = U(\boldsymbol{r}). \tag{A.2}$$

The resulting Schrödinger-equation (neglecting spin) becomes

$$\hat{\mathrm{H}}\phi(\boldsymbol{r}) = \left[-\frac{1}{2}\nabla^2 + U(\boldsymbol{r})\right]\phi(\boldsymbol{r}) = \varepsilon\phi(\boldsymbol{r}). \tag{A.3}$$

Then, *Bloch's theorem* states that the eigenstates of eq. (A.3) are of the form

$$\phi_{n\boldsymbol{k}}(\boldsymbol{r}) = \mathrm{e}^{\mathrm{i}\boldsymbol{k}\boldsymbol{r}} u_{n\boldsymbol{k}}(\boldsymbol{r}), \tag{A.4}$$

where $u_{n\boldsymbol{k}}(\boldsymbol{r}) = u_{n\boldsymbol{k}}(\boldsymbol{r} + \boldsymbol{R})$ has the same periodicity as the potential [29]. Equation (A.4) define the so-called *Bloch states*, they are labeled by a, a priori, continuous wave-vector $\boldsymbol{k}$ and a discrete quantum index n.

A.2.1. Born-von Karman boundary condition

Instead of the infinite crystal, one usually defines a finite, but large volume commensurate with the primitive cell of the underlying Bravais lattice and considers the boundary condition

$$\phi(\boldsymbol{r} + N_i \boldsymbol{a}_i) = \phi(\boldsymbol{r}) \quad \text{for} \quad i = 1, 2, 3. \tag{A.5}$$

This is known as the *Born-von-Karman boundary condition* and

$$V = N_1 N_2 N_3 \Omega,\ N_i \in \mathbb{Z} \tag{A.6}$$

is the *Born-von-Karman volume*. Applying this condition restricts the continuous $\boldsymbol{k}$ to a discrete set defined by

$$\boldsymbol{k} = \sum_{i=1}^{3} \frac{m_i}{N_i} \boldsymbol{b}_i \quad \text{for} \quad m_i \in \mathbb{Z}. \tag{A.7}$$

In the following we will denote only the fractional part of eq. (A.7), i.e. the part within the reciprocal unit cell, with $\boldsymbol{k}$ and the integer part is described by a reciprocal lattice vector $\boldsymbol{G}$.

Using the BKB and the Bloch ansatz, the Schrödinger equation can be restated for each k-vector in the reciprocal unit cell in terms of the periodic part alone

$$\hat{\mathrm{H}}_{\boldsymbol{k}} u_{\boldsymbol{k}}(\boldsymbol{r}) = \left((-i\nabla + \boldsymbol{k})^2 + U(\boldsymbol{r})\right) u_{\boldsymbol{k}}(\boldsymbol{r}) = \varepsilon_{\boldsymbol{k}} u_{\boldsymbol{k}}(\boldsymbol{r}). \tag{A.8}$$

A.3. Properties of a Bloch wave

A.3.1. General properties

In the following we state the properties of a Bloch wave in a system with BKB conditions with respect to translations in $\boldsymbol{r}$ and $\boldsymbol{k}$ (see chap. 8 of ref. [29]). The Bloch functions satisfy

$$\phi_{n\boldsymbol{k}}(\boldsymbol{r} + \boldsymbol{R}) = \mathrm{e}^{\mathrm{i}\boldsymbol{k}\boldsymbol{R}} \phi_{n\boldsymbol{k}}(\boldsymbol{r}) \quad \text{and} \quad \phi_{n\boldsymbol{k}+\boldsymbol{G}}(\boldsymbol{r}) = \phi_{n\boldsymbol{k}}(\boldsymbol{r}), \tag{A.9}$$

while the periodic part behaves as

$$u_{n\boldsymbol{k}}(\boldsymbol{r} + \boldsymbol{R}) = u_{n\boldsymbol{k}}(\boldsymbol{r}) \quad \text{and} \quad u_{n\boldsymbol{k}+\boldsymbol{G}}(\boldsymbol{r}) = \mathrm{e}^{-\mathrm{i}\boldsymbol{G}\boldsymbol{r}} u_{n\boldsymbol{k}}(\boldsymbol{r}). \tag{A.10}$$

The eigenvalues do not change for different $\boldsymbol{G}$-components

$$\epsilon_{n\boldsymbol{k}+\boldsymbol{G}} = \epsilon_{n\boldsymbol{k}}. \tag{A.11}$$

Any function $f(\boldsymbol{r})$ can be used to construct a corresponding Bloch function by

$$f_{\boldsymbol{k}}^{\mathrm{Bloch}}(\boldsymbol{r}) = \sum_{\boldsymbol{R}} \mathrm{e}^{\mathrm{i}\boldsymbol{k}\boldsymbol{R}} f(\boldsymbol{r} - \boldsymbol{R}). \tag{A.12}$$

A.3.2. Time reversal symmetry

The Hamiltonian eq. (A.3) is invariant under *time reversal*. Time reversal is a discrete symmetry transformation given by *time reversal operator* $\hat{\mathrm{T}}$. For a spin-less electron $\hat{\mathrm{T}}$ is equal to the operator of the complex conjugation $\hat{\mathrm{C}}$ (see chap. 11.4 of ref. [30]):

$$\hat{\mathrm{T}} = \hat{\mathrm{C}} \quad \text{and} \quad \hat{\mathrm{T}}^{-1} = \hat{\mathrm{C}}. \tag{A.13}$$

Applying this transformation to the $\boldsymbol{k}$-dependent Hamiltonian of eq. (A.8) reveals a connection between the solutions at $\boldsymbol{k}$ and $-\boldsymbol{k}$, namely

$$\hat{\mathrm{T}}^{-1}\hat{\mathrm{H}}_{\boldsymbol{k}}\hat{\mathrm{T}} = \hat{\mathrm{H}}_{-\boldsymbol{k}}. \tag{A.14}$$

From this it follows that

$$\hat{\mathrm{H}}_{-\boldsymbol{k}}\left(\hat{\mathrm{T}}^{-1}u_{\boldsymbol{k}}\right) = \epsilon_{\boldsymbol{k}}\left(\hat{\mathrm{T}}^{-1}u_{\boldsymbol{k}}\right) \tag{A.15}$$

resulting in the useful relations

$$u_{n-\boldsymbol{k}} = u^*_{n\boldsymbol{k}} \leftrightarrow \phi_{n,-\boldsymbol{k}} = \phi^*_{n\boldsymbol{k}} \tag{A.16a}$$

and

$$\varepsilon_{\boldsymbol{k}} = \varepsilon_{-\boldsymbol{k}}. \tag{A.16b}$$

The spin-1/2 case

Though the present work does not deal with the explicit spin treatment, we will note here the behaviour of a non-relativistic spin-1/2-dependent $\hat{\mathrm{H}}_{\boldsymbol{k}}$ under time reversal. A usual approximate form derived from the Dirac equation is

$$\hat{\mathrm{H}} = \frac{1}{2}\hat{\boldsymbol{p}}^2 + U(\boldsymbol{r}) - \frac{1}{8}\hat{\boldsymbol{p}}^4 + \frac{1}{8}\nabla^2 U(\boldsymbol{r}) + \frac{1}{4}\left(\nabla U(\boldsymbol{r}) \times \hat{\boldsymbol{p}}\right)\sigma, \tag{A.17}$$

where σ is the "vector" of Pauli matrices. The corresponding Bloch Hamiltonian is

$$\hat{\mathrm{H}}_{\boldsymbol{k}} = \frac{1}{2}\left(\hat{\boldsymbol{p}} + \boldsymbol{k}\right)^2 + U(\boldsymbol{r}) - \frac{1}{8}\left(\hat{\boldsymbol{p}} + \boldsymbol{k}\right)^4 + \frac{1}{8}\nabla^2 U(\boldsymbol{r}) + \frac{1}{4}\left(\nabla U(\boldsymbol{r}) \times (\hat{\boldsymbol{p}} + \boldsymbol{k})\right)\sigma. \tag{A.18}$$

The time reversal operator can then be defined as (see chap. 11.4.2.3 of ref. [30])

$$\hat{\mathrm{T}} = -\mathrm{i}\boldsymbol{\sigma}_y\hat{\mathrm{C}} \quad \text{and} \quad \hat{\mathrm{T}}^{-1} = \mathrm{i}\boldsymbol{\sigma}_y\hat{\mathrm{C}}, \tag{A.19}$$

where now also the Pauli matrix $\boldsymbol{\sigma}_y$

$$\boldsymbol{\sigma}_y = \begin{pmatrix} 0 & -\mathrm{i} \\ \mathrm{i} & 0 \end{pmatrix} \tag{A.20}$$

enters. It can then be shown that eqs. (A.14) and (A.15) are still valid for eq. (A.18). It then follows, that to each Bloch function at wave-vector $\boldsymbol{k}$

$$\Phi_{n\boldsymbol{k}}(\boldsymbol{r}) = \begin{pmatrix} \phi_{n\boldsymbol{k}\uparrow}(\boldsymbol{r}) \\ \phi_{n\boldsymbol{k}\downarrow}(\boldsymbol{r}) \end{pmatrix} = \mathrm{e}^{\mathrm{i}\boldsymbol{k}\boldsymbol{r}} \begin{pmatrix} u_{n\boldsymbol{k}\uparrow}(\boldsymbol{r}) \\ u_{n\boldsymbol{k}\downarrow}(\boldsymbol{r}) \end{pmatrix} \tag{A.21}$$

the Bloch function at wave-vector $-\boldsymbol{k}$ is related as

$$\Phi_{n-\boldsymbol{k}}(\boldsymbol{r}) = \begin{pmatrix} \phi_{n-\boldsymbol{k}\uparrow}(\boldsymbol{r}) \\ \phi_{n-\boldsymbol{k}\downarrow}(\boldsymbol{r}) \end{pmatrix} = \begin{pmatrix} \phi^*_{n\boldsymbol{k}\downarrow}(\boldsymbol{r}) \\ -\phi^*_{n\boldsymbol{k}\uparrow}(\boldsymbol{r}) \end{pmatrix} \tag{A.22}$$

while both are eigenstates to the same energy $\varepsilon_{n\boldsymbol{k}}$.

B. Lattice Fourier transformation

In this chapter the conventions for the Fourier transform in the context of a periodic crystal (lattice Fourier transform) are presented. They agree with the definitions given in [10, 17].

B.1. Local and non-local functions

The lattice Fourier transform of an arbitrary local function can be defined as

$$F_{\boldsymbol{G}}(\boldsymbol{q}) = \frac{1}{V}\int_V f(\boldsymbol{r})\,\mathrm{e}^{-\mathrm{i}(\boldsymbol{q}+\boldsymbol{G})\boldsymbol{r}}\,\mathrm{d}^3\boldsymbol{r}\,, \tag{B.1a}$$

and the corresponding inverse transform is given by

$$f(\boldsymbol{r}) = \sum_{\boldsymbol{q},\boldsymbol{G}} F_{\boldsymbol{G}}(\boldsymbol{q})\mathrm{e}^{\mathrm{i}(\boldsymbol{q}+\boldsymbol{G})\boldsymbol{r}}. \tag{B.1b}$$

Similarly, for a non-local function depending on two positions the lattice Fourier transform is chosen to be

$$F_{\boldsymbol{G}\boldsymbol{G}'}(\boldsymbol{q},\boldsymbol{q}') = \frac{1}{V}\iint \mathrm{d}^3r\,\mathrm{d}^3r'\;\mathrm{e}^{-\mathrm{i}(\boldsymbol{q}+\boldsymbol{G})\boldsymbol{r}} f(\boldsymbol{r},\boldsymbol{r}')\mathrm{e}^{\mathrm{i}(\boldsymbol{q}'+\boldsymbol{G}')\boldsymbol{r}'} \tag{B.2a}$$

and its inverse then given by

$$\tag{B.2b}$$

$$f(\boldsymbol{r},\boldsymbol{r}') = \frac{1}{V}\sum_{\boldsymbol{q},\boldsymbol{G}}\sum_{\boldsymbol{q}',\boldsymbol{G}'} \mathrm{e}^{\mathrm{i}(\boldsymbol{q}+\boldsymbol{G})\boldsymbol{r}} f_{\boldsymbol{G},\boldsymbol{G}'}(\boldsymbol{q},\boldsymbol{q}')\mathrm{e}^{-\mathrm{i}(\boldsymbol{q}'+\boldsymbol{G}')\boldsymbol{r}'}. \tag{B.2c}$$

B.2. Periodic function

Formulas (B.1) and (B.2) simplify in the case that the functions are periodic with respect to a translation with a lattice vector.

For a local function satisfying $f(\boldsymbol{r}+\boldsymbol{R}) = f(\boldsymbol{r})$, only Fourier coefficients with $\boldsymbol{q} = 0$ will be non-vanishing.

$$\begin{aligned} f(\boldsymbol{r}) &= \frac{1}{V}\sum_{\boldsymbol{q}\boldsymbol{G}} F_{\boldsymbol{G}}(\boldsymbol{q})\mathrm{e}^{\mathrm{i}(\boldsymbol{q}+\boldsymbol{G})\boldsymbol{r}} \overset{!}{=} f(\boldsymbol{r}+\boldsymbol{R}) = \frac{1}{V}\sum_{\boldsymbol{q}\boldsymbol{G}} F_{\boldsymbol{G}}(\boldsymbol{q})\mathrm{e}^{\mathrm{i}(\boldsymbol{q}+\boldsymbol{G})\boldsymbol{r}}\mathrm{e}^{\mathrm{i}\boldsymbol{q}\boldsymbol{R}} \\ &= \frac{1}{V}\sum_{\boldsymbol{G}} F_{\boldsymbol{G}}(0)\mathrm{e}^{\mathrm{i}\boldsymbol{G}\boldsymbol{r}} \end{aligned} \tag{B.3}$$

A consequence is that the integral

$$\begin{aligned}\int \mathrm{d}r\, f(\boldsymbol{r})\mathrm{e}^{-\mathrm{i}\boldsymbol{K}\boldsymbol{r}} &= \frac{1}{V}\sum_{\boldsymbol{G}} f(0,\boldsymbol{G}) \int \mathrm{d}r\, \mathrm{e}^{\mathrm{i}(\boldsymbol{G}-\boldsymbol{K})\boldsymbol{r}} \\ &= \frac{1}{V}\sum_{\boldsymbol{G}} f(0,\boldsymbol{G})\delta_{\boldsymbol{G},\boldsymbol{K}} V = \sum_{\boldsymbol{G}} f(0,\boldsymbol{G})\delta_{\boldsymbol{G},\boldsymbol{K}} \\ &= f(0,\boldsymbol{K})\end{aligned} \tag{B.4}$$

is only non-vanishing if $\boldsymbol{K}$ is a reciprocal lattice vector. In a similar fashion it can be shown that the lattice Fourier transform of a non-local function satisfying $f(\boldsymbol{r}+\boldsymbol{R},\boldsymbol{r}'+\boldsymbol{R}) = f(\boldsymbol{r},\boldsymbol{r}')$ only depends on one $\boldsymbol{q}$ variable instead of two

$$\begin{aligned} f(\boldsymbol{r},\boldsymbol{r}') &= \frac{1}{V}\sum_{\boldsymbol{q},\boldsymbol{G}}\sum_{\boldsymbol{q}',\boldsymbol{G}'} \mathrm{e}^{\mathrm{i}(\boldsymbol{q}+\boldsymbol{G})\boldsymbol{r}} F_{\boldsymbol{G}\boldsymbol{G}'}(\boldsymbol{q},\boldsymbol{q}')\mathrm{e}^{-\mathrm{i}(\boldsymbol{q}'+\boldsymbol{G}')\boldsymbol{r}'} \\ \overset{!}{=} f(\boldsymbol{r}+\boldsymbol{R},\boldsymbol{r}'+\boldsymbol{R}) &= \frac{1}{V}\sum_{\boldsymbol{q},\boldsymbol{G}}\sum_{\boldsymbol{q}',\boldsymbol{G}'} \mathrm{e}^{\mathrm{i}(\boldsymbol{q}+\boldsymbol{G})\boldsymbol{r}} F_{\boldsymbol{G}\boldsymbol{G}'}(\boldsymbol{q},\boldsymbol{q}')\mathrm{e}^{-\mathrm{i}(\boldsymbol{q}'+\boldsymbol{G}')\boldsymbol{r}'}\mathrm{e}^{\mathrm{i}(\boldsymbol{q}-\boldsymbol{q}')\boldsymbol{R}} \\ &= \frac{1}{V}\sum_{\boldsymbol{q}}\sum_{\boldsymbol{G},\boldsymbol{G}'} \mathrm{e}^{\mathrm{i}(\boldsymbol{q}+\boldsymbol{G})\boldsymbol{r}} F_{\boldsymbol{G}\boldsymbol{G}'}(\boldsymbol{q},\boldsymbol{q})\mathrm{e}^{-\mathrm{i}(\boldsymbol{q}+\boldsymbol{G}')\boldsymbol{r}'} .\end{aligned} \tag{B.5}$$

B.3. Fourier transform in time

The Fourier transform between the time and (angular) frequency domain is chosen to be

$$F(\omega) = \int f(t)\mathrm{e}^{\mathrm{i}\omega t}\,\mathrm{d}t \tag{B.6a}$$

with the corresponding inverse transform

$$f(t) = \frac{1}{2\pi}\int F(\omega)\mathrm{e}^{-\mathrm{i}\omega t}\,\mathrm{d}\omega\,. \tag{B.6b}$$

C. The (L)APW+lo basis

`Exciting` employs the *augmented plane wave* method (APW) in which the unit cell is partitioned into spherical regions centered around each atom, the so called *muffin-tins*, and an interstitial region. Within the interstitial region plane waves are used as basis functions, while atomic-like functions are used inside the muffin-tins. Each augmented plane wave is thus defined as

$$\phi^{\text{apw}}_{\boldsymbol{k}+\boldsymbol{G}}(\boldsymbol{r}) = \begin{cases} \frac{1}{\sqrt{V}} \mathrm{e}^{\mathrm{i}(\boldsymbol{k}+\boldsymbol{G})\boldsymbol{r}} & , \boldsymbol{r} \in \text{interstitial} \\ \sum\limits_{\alpha,l,m} f^{\alpha,lm}_{\boldsymbol{k}+\boldsymbol{G}}(r_\alpha) Y_{lm}(\hat{\boldsymbol{r}}_\alpha) & , \boldsymbol{r} \in \text{muffin-tin} \end{cases} . \tag{C.1}$$

Here, $\boldsymbol{r}_\alpha = \boldsymbol{r} - \boldsymbol{R}_\alpha$ and $\boldsymbol{R}_\alpha$ is the center of the muffin-tin sphere around atom α. The coefficients $f^{\alpha,lm}_{\boldsymbol{k}+\boldsymbol{G}}(r_\alpha)$ are given in terms the of real-valued radial functions $u^\alpha_{lp}(r_\alpha, E_l)$ and the matching coefficients $A^\alpha_{lmp}(\boldsymbol{k}+\boldsymbol{G})$:

$$f^{\alpha,lm}_{\boldsymbol{k}+\boldsymbol{G}}(r_\alpha) = \sum_{p=0}^{p_{\max}} A^\alpha_{lmp}(\boldsymbol{k}+\boldsymbol{G}) u^\alpha_{lp}(r_\alpha, E_l). \tag{C.2}$$

Within the muffin-tin regions the Kohn-Sham potential is assumed to be spherically symmetric and the *radial wave function* $u^\alpha_l(r_\alpha, E_l)$ is calculated by the radial, scalar-relativistic Schrödinger equation for a fixed *linearization energy* E_l [31]. The radial functions $u^\alpha_{lp}(r_\alpha, E_l)$ are the p-th energy derivate of the radial wave functions and taking $p_{\max} = 1$ yields the so-called *linearized augmented plane wave* method (LAPW). The matching coefficients are chosen such that the basis functions are continuous up to the order $p_{\max}$.

In addition to the APW functions `exciting` supports so-called *local orbitals*, which are atomic-like functions within the muffin-tins

$$\phi^{\text{lo}}_L(\boldsymbol{r}) = \begin{cases} 0 & , \boldsymbol{r} \in \text{interstitial} \\ v^\alpha_L(r_\alpha) Y_{lm}(\hat{\boldsymbol{r}}_\alpha) & , \boldsymbol{r} \in \text{muffin-tin of atom } \alpha. \end{cases} \tag{C.3}$$

The $v^\alpha_L(r_\alpha)$ are also combinations of the radial functions $u^\alpha_{lp}(r_\alpha, E_b)$ and matching coefficients A^α_b

$$v^\alpha_L(r) = \sum_{b=0}^{p_{\max}} A^\alpha_b u^\alpha_{lp_b}(r, E_b). \tag{C.4}$$

The matching coefficients are chosen such that the derivatives of the local orbital are zero up to the $(p_{\max} - 1)$-th order and such that it is normalized within the muffin-tin. Mathematically, a Bloch basis function is constructed from each local orbital according to

$$\phi^{\text{lo}}_{\boldsymbol{k},L}(\boldsymbol{r}) = \sum_{\boldsymbol{R}} \mathrm{e}^{\mathrm{i}\boldsymbol{R}\boldsymbol{k}} \phi^{\text{lo}}_L(\boldsymbol{r} - \boldsymbol{R}), \tag{C.5}$$

but in practice only integrals over the first unit cell are calculated in which case only eq. (C.3) is needed. Here, the index L contains the indices $\{l, m, \alpha\}$ and the matching order p_{max}. With the inclusion of local orbitals the overall flexibility of the basis set is increased, especially with respect to the description of low lying semi-core states. The expansion of the Bloch wave functions within the (L)APW+lo basis is thus

$$\phi_{n\boldsymbol{k}}(\boldsymbol{r}) = \sum_{\boldsymbol{G}} c_{n\boldsymbol{k}+\boldsymbol{G}} \phi^{\mathrm{apw}}_{\boldsymbol{k}+\boldsymbol{G}} + \sum_{L} c_{n\boldsymbol{k},L} \phi^{\mathrm{lo}}_{\boldsymbol{k},L}(\boldsymbol{r}). \tag{C.6}$$

D. Plane-wave matrix elements

The key quantity to compute for the setup of the BSE Hamiltonian are the plane-wave matrix elements (PWE) $M_{mn\boldsymbol{k}}(\boldsymbol{G},\boldsymbol{q})$, as seen in section 3.3. In the following, we first note some of their general properties in appendix D.1, then discuss the optical limit in appendix D.2, and go into detail about how they are computed in the (L)APW+lo basis set in appendix D.3.

D.1. General properties

The matrix elements of a (non-normalized) plane wave and two Bloch states (neglecting spin) can be written as

$$\left\langle f\boldsymbol{k}_f\middle|\mathrm{e}^{-\mathrm{i}(\boldsymbol{G}+\boldsymbol{q})\boldsymbol{r}}\middle|i\boldsymbol{k}_i\right\rangle = \delta_{\lfloor \boldsymbol{k}_f-\boldsymbol{k}_i+\boldsymbol{q}\rfloor_{1^{\mathrm{st}}\,\mathrm{BZ}},0}\, M_{fi\boldsymbol{k}_f}(\boldsymbol{G},\boldsymbol{q}), \tag{D.1}$$

where $\delta_{\lfloor \boldsymbol{k}_f-\boldsymbol{k}_i+\boldsymbol{q}\rfloor_{1^{\mathrm{st}}\,\mathrm{BZ}},0}$ denotes that the element is only non-zero if $\boldsymbol{k}_i = \boldsymbol{k}_f + \boldsymbol{q}$ apart from some reciprocal lattice vector. From the definition above it follows directly that

$$M_{fi\boldsymbol{k}_f}(\boldsymbol{G},\boldsymbol{q}) = M^*_{if\boldsymbol{k}_i}(-\boldsymbol{G},-\boldsymbol{q}). \tag{D.2}$$

Using the time reversal symmetry of the Bloch states $|i-\boldsymbol{k}\rangle = \left|(i\boldsymbol{k})^*\right\rangle$, the identity

$$M_{fi\boldsymbol{k}_f}(\boldsymbol{G},\boldsymbol{q}) = M_{if-\boldsymbol{k}_i}(\boldsymbol{G},\boldsymbol{q}) \tag{D.3}$$

is found.

D.2. Optical limit of the plane wave matrix elements

In order to take the limit $\boldsymbol{q} \to 0$ of the plane-wave matrix element $\langle f\boldsymbol{k}_\mathrm{f}|\mathrm{e}^{-\mathrm{i}(\boldsymbol{G}+\boldsymbol{q})\boldsymbol{r}}|i\boldsymbol{k}_\mathrm{f}+\boldsymbol{q}\rangle$ at $\boldsymbol{G}=0$ some care has to be taken. The expansion for small $\boldsymbol{q}$ is given by

$$\begin{aligned}\langle f\boldsymbol{k}_\mathrm{f}|\mathrm{e}^{-\mathrm{i}\boldsymbol{q}\boldsymbol{r}}|i\boldsymbol{k}_\mathrm{f}+\boldsymbol{q}\rangle &= \langle f\boldsymbol{k}_\mathrm{f}|\, 1-\mathrm{i}\boldsymbol{q}\boldsymbol{r}+\ldots \Big(|i\boldsymbol{k}_\mathrm{f}\rangle + \boldsymbol{q}\nabla_{\boldsymbol{k}}\,|i\boldsymbol{k}\rangle\,|_{\boldsymbol{k}_\mathrm{f}} + \ldots\Big)\\ &= \delta_{fi} + \mathrm{i}\boldsymbol{q}\langle f\boldsymbol{k}_\mathrm{f}|-\boldsymbol{r}|i\boldsymbol{k}_\mathrm{f}\rangle + \boldsymbol{q}\langle f\boldsymbol{k}_\mathrm{f}|\left(\nabla_{\boldsymbol{k}}\,|i\boldsymbol{k}\rangle\right)_{\boldsymbol{k}_\mathrm{f}} + O(\boldsymbol{q}^2).\\ &\approx \delta_{fi} + \mathrm{i}\boldsymbol{q}\langle f\boldsymbol{k}_\mathrm{f}|-\boldsymbol{r}|i\boldsymbol{k}_\mathrm{f}\rangle\end{aligned} \tag{D.4}$$

If the potential part of the one-particle Hamiltonian is *local*, the usual canonical commutation relations hold

$$\left[\hat{\mathrm{r}}_i,\hat{\mathrm{p}}_j\right] = \mathrm{i}\delta_{ij} \tag{D.5a}$$

$$\left[\hat{\mathrm{h}}, \hat{\boldsymbol{r}}\right] = -\mathrm{i}\hat{\boldsymbol{p}}, \tag{D.5b}$$

which enable us to express the $\boldsymbol{r}$ expectation value in (D.4) in terms of momentum matrix elements

$$\langle f\boldsymbol{k}_\mathrm{f}|-\boldsymbol{r}|i\boldsymbol{k}_\mathrm{f}\rangle = \mathrm{i}\frac{\langle f\boldsymbol{k}_\mathrm{f}|\boldsymbol{p}|i\boldsymbol{k}_\mathrm{f}\rangle}{\epsilon_{f\boldsymbol{k}_\mathrm{f}}-\epsilon_{i\boldsymbol{k}_\mathrm{f}}} =: \boldsymbol{D}_{fi\boldsymbol{k}_\mathrm{f}}. \tag{D.6}$$

The $\boldsymbol{D}_{fi\boldsymbol{k}_\mathrm{f}}$ are the dipole operator matrix elements for electronic transitions. Plugging (D.6) into (D.4) yields

$$M_{fi\boldsymbol{k}_\mathrm{f}}(0,\boldsymbol{q}) \overset{q\ll 1}{=} \delta_{fi} + \mathrm{i}\boldsymbol{q}^\mathrm{T}\boldsymbol{D}_{fi\boldsymbol{k}_\mathrm{f}}(1-\delta_{fi}). \tag{D.7}$$

D.3. Computation in the (L)APW+lo basis

The expressions for the PEWs in terms of the (L)APW+lo basis functions are documented in detail in Ref. [11], chapter 8.2. In the following, we note the main results and subsequently point out necessary changes to compute the modified plane-wave matrix elements $N_{mn\boldsymbol{k}}(\boldsymbol{G},\boldsymbol{q})$ (3.43) needed for the construction of the coupling block of the screened Coulomb interaction (3.42).

D.3.1. Plane-wave matrix elements

In terms of the (L)APW+lo basis functions [see eqs. (C.1), (C.3) and (C.6)] the element

$$M_{nm\boldsymbol{k}'}(\boldsymbol{G},\boldsymbol{q}) = \langle \phi_{n\boldsymbol{k}'}|\mathrm{e}^{-\mathrm{i}(\boldsymbol{G}+\boldsymbol{q})\boldsymbol{r}}|\phi_{m\boldsymbol{k}''}\rangle\, \delta_{\lfloor \boldsymbol{k}'-\boldsymbol{k}''+\boldsymbol{q}\rfloor_{1^\mathrm{st}\,\mathrm{BZ}},0} \tag{D.8}$$

can be written as

$$\begin{aligned} M_{nm\boldsymbol{k}'}(\boldsymbol{G},\boldsymbol{q})/N_{\boldsymbol{k}} = & \sum_{\boldsymbol{G}'\boldsymbol{G}''} c^*_{n\boldsymbol{k}'+\boldsymbol{G}'} c_{m\boldsymbol{k}''+\boldsymbol{G}''} M_{\boldsymbol{G}'\boldsymbol{G}''\boldsymbol{k}'}(\boldsymbol{G},\boldsymbol{q}) \\ & + \sum_{\boldsymbol{G}'L''} c^*_{n\boldsymbol{k}'+\boldsymbol{G}'} c_{m\boldsymbol{k}'',L''} M_{\boldsymbol{G}'L''\boldsymbol{k}'}(\boldsymbol{G},\boldsymbol{q}) \\ & + \sum_{L'\boldsymbol{G}''} c^*_{n\boldsymbol{k}',L'} c_{m\boldsymbol{k}''+\boldsymbol{G}''} M_{L'\boldsymbol{G}''\boldsymbol{k}'}(\boldsymbol{G},\boldsymbol{q}) \\ & + \sum_{L'L''} c^*_{n\boldsymbol{k}',L'} c_{m\boldsymbol{k}'',L''} M_{L'L''\boldsymbol{k}'}(\boldsymbol{G},\boldsymbol{q}) \end{aligned}, \tag{D.9}$$

where the integrals over the unit cell between the two types of basis functions are

$$M_{\boldsymbol{G}'\boldsymbol{G}''\boldsymbol{k}'}(\boldsymbol{G},\boldsymbol{q}) = \left\langle \phi_{\boldsymbol{k}'+\boldsymbol{G}'}\middle|\mathrm{e}^{-\mathrm{i}(\boldsymbol{G}+\boldsymbol{q})\boldsymbol{r}}\middle|\phi_{\boldsymbol{k}''+\boldsymbol{G}''}\right\rangle_\Omega \tag{D.10a}$$

$$M_{\boldsymbol{G}'L''\boldsymbol{k}'}(\boldsymbol{G},\boldsymbol{q}) = \left\langle \phi_{\boldsymbol{k}'+\boldsymbol{G}'}\middle|\mathrm{e}^{-\mathrm{i}(\boldsymbol{G}+\boldsymbol{q})\boldsymbol{r}}\middle|\phi_{\boldsymbol{k}'',L''}\right\rangle_\Omega \tag{D.10b}$$

$$M_{L'\boldsymbol{G}''\boldsymbol{k}'}(\boldsymbol{G},\boldsymbol{q}) = \left\langle \phi_{\boldsymbol{k}',L'}\middle|\mathrm{e}^{-\mathrm{i}(\boldsymbol{G}+\boldsymbol{q})\boldsymbol{r}}\middle|\phi_{\boldsymbol{k}''+\boldsymbol{G}''}\right\rangle_\Omega \tag{D.10c}$$

$$M_{L'L''\boldsymbol{k}'}(\boldsymbol{G},\boldsymbol{q}) = \left\langle \phi_{\boldsymbol{k}',L'} \middle| \mathrm{e}^{-\mathrm{i}(\boldsymbol{G}+\boldsymbol{q})\boldsymbol{r}} \middle| \phi_{\boldsymbol{k}'',L''} \right\rangle_{\Omega} . \tag{D.10d}$$

The integrals above can be split into two contribution, stemming from the interstitial and the muffin-tin part of the unit cell

$$M_{ab\boldsymbol{k}}(\boldsymbol{G},\boldsymbol{q}) = M^{\mathrm{I}}_{ab\boldsymbol{k}}(\boldsymbol{G},\boldsymbol{q}) + M^{\mathrm{MT}}_{ab\boldsymbol{k}}(\boldsymbol{G},\boldsymbol{q}), \tag{D.11}$$

where $a, b \in \left\{\boldsymbol{G}', \boldsymbol{G}'', L', L''\right\}$. In the interstitial region, only the plane-wave part of the APW functions is non-zero, so that only $M^{\mathrm{I}}_{\boldsymbol{G}'\boldsymbol{G}''\boldsymbol{k}'}(\boldsymbol{G},\boldsymbol{q})$ needs to be calculated. Using the lattice-theta function $\Theta_{\mathrm{I}}(\boldsymbol{r})$

$$\Theta_{\mathrm{I}}(\boldsymbol{r}) = \begin{cases} 1 & , \boldsymbol{r} \in \text{interstitial} \\ 0 & , \text{else} \end{cases} , \tag{D.12}$$

it is given by

$$\begin{aligned} M^{\mathrm{I}}_{\boldsymbol{G}'\boldsymbol{G}''\boldsymbol{k}'}(\boldsymbol{G},\boldsymbol{q}) &= \frac{1}{\Omega}\int_{\Omega} \Theta_{\mathrm{I}}(\boldsymbol{r})\mathrm{e}^{-\mathrm{i}\left(\boldsymbol{k}'+\boldsymbol{G}'\right)\boldsymbol{r}}\mathrm{e}^{-\mathrm{i}(\boldsymbol{q}+\boldsymbol{G})\boldsymbol{r}}\mathrm{e}^{\mathrm{i}\left(\boldsymbol{k}''+\boldsymbol{G}''\right)\boldsymbol{r}}\,\mathrm{d}^3\boldsymbol{r} \\ &= \frac{1}{\Omega}\int_{\Omega} \Theta_{\mathrm{I}}(\boldsymbol{r})\mathrm{e}^{-\mathrm{i}\left(\boldsymbol{G}'-\boldsymbol{G}''+\boldsymbol{G}\right)\boldsymbol{r}}\,\mathrm{d}^3\boldsymbol{r} = \tilde{\Theta}_{\mathrm{I}}(\boldsymbol{G}'-\boldsymbol{G}''+\boldsymbol{G}), \end{aligned} \tag{D.13}$$

where $\tilde{\Theta}_{\mathrm{I}}$ is the lattice Fourier transform of Θ_{I}. In the muffin-tin regions all four integrals eq. (D.10) are non-vanishing. After expanding the exponential $\mathrm{e}^{-\mathrm{i}(\boldsymbol{q}+\boldsymbol{G})\boldsymbol{r}}$ in terms of spherical harmonics Y_{lm} and spherical Bessel functions of first kind j_l according to

$$\mathrm{e}^{-\mathrm{i}(\boldsymbol{q}+\boldsymbol{G})\boldsymbol{r}} = 4\pi\sum_{lm}(-i)^l j_l(|\boldsymbol{q}+\boldsymbol{G}|r)Y_{lm}(\hat{\boldsymbol{r}})Y^*_{lm}(\widehat{\boldsymbol{q}+\boldsymbol{G}}), \tag{D.14}$$

the APW-APW elements are found to be

$$\begin{aligned} M^{\mathrm{MT}}_{\boldsymbol{G}'\boldsymbol{G}''\boldsymbol{k}'}(\boldsymbol{G},\boldsymbol{q}) = 4\pi\sum_{\alpha}\mathrm{e}^{-\mathrm{i}(\boldsymbol{G}+\boldsymbol{q})\boldsymbol{R}_{\alpha}}\sum_{l'm'p'}\left(A^{\alpha}_{l'm'p'}(\boldsymbol{k}'+\boldsymbol{G}')\right)^* \\ \times\sum_{l''m''p''}A^{\alpha}_{l''m''p''}(\boldsymbol{k}''+\boldsymbol{G}'')X^{\alpha}_{l'm'p',l''m''p''}(\boldsymbol{q}+\boldsymbol{G}), \end{aligned} \tag{D.15a}$$

where X and R are auxiliary quantities defined as

$$X^{\alpha}_{l'm'p',l''m''p''}(\boldsymbol{q}+\boldsymbol{G}) = \sum_{l}(-\mathrm{i})^l R^{\alpha}_{l'p',l''p'',l}(\boldsymbol{q}+\boldsymbol{G})\sum_{m}Y^*_{lm}(\widehat{\boldsymbol{q}+\boldsymbol{G}})C^{l'm'}_{lm,l''m''} \tag{D.15b}$$

and

$$R^{\alpha}_{l'p',l''p'',l}(\boldsymbol{q}+\boldsymbol{G}) = \int_0^{R^{\mathrm{MT}}_{\alpha}} u^{\alpha}_{l'p'}(r)j_l(|\boldsymbol{q}+\boldsymbol{G}|r)u^{\alpha}_{l''p''}(r)r^2\,\mathrm{d}r\,. \tag{D.15c}$$

Here, the C are the so-called Gaunt coefficients

$$C^{l'm'}_{lm,l''m''} = \iint Y^*_{l'm'}(\hat{\boldsymbol{r}})Y_{lm}(\hat{\boldsymbol{r}})Y_{l''m''}(\hat{\boldsymbol{r}})\,\mathrm{d}\Omega\,. \tag{D.16}$$

The APW-LO matrix elements are given by

$$M^{\mathrm{MT}}_{\boldsymbol{G}'L''\boldsymbol{k}}(\boldsymbol{G},\boldsymbol{q}) = 4\pi \sum_{\alpha} \mathrm{e}^{-\mathrm{i}(\boldsymbol{G}+\boldsymbol{q})\boldsymbol{R}_\alpha} \sum_{l'm'p'} \left(A^{\alpha}_{l'm'p'}(\boldsymbol{k}'+\boldsymbol{G}')\right)^{*} X^{\alpha}_{l'm'p',L''}(\boldsymbol{q}+\boldsymbol{G}), \tag{D.17a}$$

with

$$X^{\alpha}_{l'm'p',L''}(\boldsymbol{q}+\boldsymbol{G}) = \sum_{l} (-\mathrm{i})^{l} R^{\alpha}_{l'p',L'',l}(\boldsymbol{q}+\boldsymbol{G}) \sum_{m} Y^{*}_{lm}(\widehat{\boldsymbol{q}+\boldsymbol{G}}) C^{l'm'}_{lm,l''m''} \tag{D.17b}$$

and

$$R^{\alpha}_{l'p',L'',l}(\boldsymbol{q}+\boldsymbol{G}) = \delta_{\alpha,\alpha''} \int_0^{R^{\mathrm{MT}}_{\alpha}} u^{\alpha}_{l'p'}(r) j_l(|\boldsymbol{q}+\boldsymbol{G}|r) v^{\alpha}_{L''}(r) r^2 \,\mathrm{d}r\,. \tag{D.17c}$$

Lastly, the LO-LO matrix elements are computed using

$$M^{\mathrm{MT}}_{L'L''\boldsymbol{k}'}(\boldsymbol{G},\boldsymbol{q}) = 4\pi \sum_{\alpha} \mathrm{e}^{-\mathrm{i}(\boldsymbol{G}+\boldsymbol{q})\boldsymbol{R}_\alpha} X^{\alpha}_{L',L''}(\boldsymbol{q}+\boldsymbol{G}), \tag{D.18a}$$

with

$$X^{\alpha}_{L',L''}(\boldsymbol{q}+\boldsymbol{G}) = \sum_{l} (-\mathrm{i})^{l} R^{\alpha}_{L',L'',l}(\boldsymbol{q}+\boldsymbol{G}) \sum_{m} Y^{*}_{lm}(\widehat{\boldsymbol{q}+\boldsymbol{G}}) C^{l'm'}_{lm,l''m''} \tag{D.18b}$$

and

$$R^{\alpha}_{L',L'',l}(\boldsymbol{q}+\boldsymbol{G}) = \delta_{\alpha,\alpha'}\delta_{\alpha,\alpha''} \int_0^{R^{\mathrm{MT}}_{\alpha}} v^{\alpha}_{L'}(r) j_l(|\boldsymbol{q}+\boldsymbol{G}|r) v^{\alpha}_{L''}(r) r^2 \,\mathrm{d}r\,. \tag{D.18c}$$

D.3.2. Modified plane-wave matrix elements

In order to calculate the modified plane-wave matrix elements

$$N_{nm\boldsymbol{k}'}(\boldsymbol{G},\boldsymbol{q}) = \left\langle \phi_{n\boldsymbol{k}'} \middle| \mathrm{e}^{-\mathrm{i}(\boldsymbol{G}+\boldsymbol{q})\boldsymbol{r}} \middle| \left(\phi_{m\boldsymbol{k}''}\right)^{*} \right\rangle \delta_{\lfloor \boldsymbol{k}'+\boldsymbol{k}''+\boldsymbol{q} \rfloor_{1^{\mathrm{st}}\,\mathrm{BZ}},0} \tag{D.19}$$

we need first to express the complex conjugate of the basis functions. Using the property of the spherical harmonics $Y^{*}_{lm}(\varphi,\theta) = (-1)^m Y_{l-m}(\varphi,\theta)$, we get

$$\phi^{\mathrm{apw}*}_{\boldsymbol{k}+\boldsymbol{G}}(\boldsymbol{r}) = \begin{cases} \dfrac{1}{\sqrt{V}} \mathrm{e}^{-\mathrm{i}(\boldsymbol{k}+\boldsymbol{G})\boldsymbol{r}} & ,\, \boldsymbol{r} \in \text{interstitial} \\ \displaystyle\sum_{\alpha,l,m} \sum_{p=0}^{p_{\max}} A^{\alpha *}_{lmp}(\boldsymbol{k}+\boldsymbol{G}) u^{\alpha}_{lp}(r_\alpha, E_l)(-1)^m Y_{l-m}(\hat{\boldsymbol{r}}_\alpha) & ,\, \boldsymbol{r} \in \text{muffin-tin} \end{cases} \tag{D.20}$$

for the APW basis functions, and

$$\phi^{\mathrm{lo}*}_{L}(\boldsymbol{r}) = \begin{cases} 0 & ,\, \boldsymbol{r} \in \text{interstitial} \\ v^{\alpha}_{L}(r_\alpha)(-1)^m Y_{l-m}(\hat{\boldsymbol{r}}_\alpha) & \boldsymbol{r} \in \text{muffin-tin of atom } \alpha. \end{cases} \tag{D.21}$$

for the local orbitals. In analogy to eq. (D.9) it is

$$N_{nm\boldsymbol{k}'}(\boldsymbol{G},\boldsymbol{q})/N_{\boldsymbol{k}} = \sum_{a\neq b} c^{*}_{n,a} c^{*}_{m,b} N_{ab\boldsymbol{k}'}(\boldsymbol{G},\boldsymbol{q}), \tag{D.22}$$

where again $a, b \in \left\{\boldsymbol{G}', \boldsymbol{G}'', L', L''\right\}$. The interstitial part (D.13) simply changes to

$$N^{\mathrm{I}}_{\boldsymbol{G}'\boldsymbol{G}''\boldsymbol{k}'}(\boldsymbol{G},\boldsymbol{q}) = \tilde{\Theta}_{\mathrm{I}}(\boldsymbol{G}' + \boldsymbol{G}'' + \boldsymbol{G}), \tag{D.23}$$

while the muffin-tin contributions (D.15a), (D.17a) and (D.18a) change according to

$$\begin{aligned} N^{\mathrm{MT}}_{\boldsymbol{G}'\boldsymbol{G}''\boldsymbol{k}'}(\boldsymbol{G},\boldsymbol{q}) = 4\pi \sum_{\alpha} \mathrm{e}^{-\mathrm{i}(\boldsymbol{G}+\boldsymbol{q})\boldsymbol{R}_\alpha} \sum_{l'm'p'} \left(A^{\alpha}_{l'm'p'}(\boldsymbol{k}' + \boldsymbol{G}')\right)^{*} \\ \times \sum_{l''m''p''} \left(A^{\alpha}_{l''m''p''}(\boldsymbol{k}'' + \boldsymbol{G}'')\right)^{*} (-1)^{m''} X^{\alpha}_{l'm'p',l''-m''p''}(\boldsymbol{q}+\boldsymbol{G}), \end{aligned} \tag{D.24a}$$

$$\begin{aligned} N^{\mathrm{MT}}_{\boldsymbol{G}'L''\boldsymbol{k}}(\boldsymbol{G},\boldsymbol{q}) = 4\pi \sum_{\alpha} \mathrm{e}^{-\mathrm{i}(\boldsymbol{G}+\boldsymbol{q})\boldsymbol{R}_\alpha} \sum_{l'm'p'} \left(A^{\alpha}_{l'm'p'}(\boldsymbol{k}' + \boldsymbol{G}')\right)^{*} \\ (-1)^{m''} X^{\alpha}_{l'm'p',L''(-m'')}(\boldsymbol{q}+\boldsymbol{G}), \end{aligned} \tag{D.24b}$$

and

$$N^{\mathrm{MT}}_{L'L''\boldsymbol{k}'}(\boldsymbol{G},\boldsymbol{q}) = 4\pi \sum_{\alpha} \mathrm{e}^{-\mathrm{i}(\boldsymbol{G}+\boldsymbol{q})\boldsymbol{R}_\alpha} (-1)^{m''} X^{\alpha}_{L',L''(-m'')}(\boldsymbol{q}+\boldsymbol{G}) \tag{D.24c}$$

respectively.

E. Dielectric response of a Kohn-Sham system

In this chapter we describe the dielectric response of a Kohn-Sham system. An expression for the dielectric matrix is derived which serves as a starting point for the BSE formalism.

E.1. Linearization of the Liouville-von-Neumann equation

For a system of independent particles, as described by the Kohn-Sham equations (2.7), the longitudinal dielectric function can be derived using the equation of motion for the density matrix operator $\hat{\rho}$ (see [2, 32]) and the procedure is sketched in the following. The time-dependent Kohn-Sham Hamiltonian including the perturbing potential can be written in terms of the unperturbed Hamiltonian plus the total perturbing effective potential as

$$\hat{\mathrm{h}}_{\mathrm{KS}}(t) = \hat{\mathrm{h}}_{\mathrm{KS}}^{(0)} + \delta V_{\mathrm{eff}}(t) = \hat{\mathrm{h}}_{\mathrm{KS}}^{(0)} + V_{\mathrm{ext}}(t) + \delta V_{\mathrm{H}}(t) + \delta V_{\mathrm{xc}}(t) \tag{E.1}$$

and the corresponding Schrödinger equation reads

$$\mathrm{i}\frac{\mathrm{d}}{\mathrm{d}t} \left|\alpha(t)\right\rangle = \hat{\mathrm{h}}_{\mathrm{KS}}(t) \left|\alpha(t)\right\rangle . \tag{E.2}$$

The time evolution of the density matrix operator

$$\hat{\rho}(t) = \sum_{\alpha}^{\mathrm{occ}} \left|\alpha(t)\right\rangle\!\left\langle\alpha(t)\right| \tag{E.3}$$

is given by the Liouville-von-Neumann equation

$$\mathrm{i}\frac{\mathrm{d}}{\mathrm{d}t}\rho\hat{(\mathrm{t})} = \left[\hat{\mathrm{h}}_{\mathrm{KS}}(t), \hat{\rho}(t)\right]. \tag{E.4}$$

Splitting also the density matrix operator into a unperturbed and a perturbed part

$$\hat{\rho}(t) = \hat{\rho}^{(0)} + \hat{\rho}^{(1)}(t) \tag{E.5}$$

allows for a linearization of (E.4) by omitting the commutator $\left[\delta V_{\mathrm{eff}}(t), \hat{\rho}^{(1)}(t)\right]$

$$\mathrm{i}\frac{\mathrm{d}}{\mathrm{d}t}\hat{\rho}^{(1)}(t) = \left[\hat{\mathrm{h}}_{\mathrm{KS}}^{(0)}, \hat{\rho}^{(1)}(t)\right] + \left[\delta V_{\mathrm{eff}}(t), \hat{\rho}^{(0)}(t)\right]. \tag{E.6}$$

Taking the matrix element of (E.6) between two eigenstates $\langle m|$ and $|n\rangle$ of the unperturbed system yields

$$\mathrm{i}\frac{\mathrm{d}}{\mathrm{d}t}\rho_{mn}^{(1)}(t) = (\varepsilon_m - \varepsilon_n)\rho_{mn}^{(1)}(t) + (f_n - f_m)\delta V_{\mathrm{eff},mn}(t). \tag{E.7}$$

Inserting the Fourier transforms of the total perturbing potential and the density matrix variation

$$\delta V_{\mathrm{eff},mn}(t) = \int \frac{\mathrm{d}\omega}{2\pi} \delta V_{\mathrm{eff},mn}(\omega) \mathrm{e}^{-\mathrm{i}(\omega+\mathrm{i}\eta)t} \tag{E.8a}$$

$$\rho^{(1)}_{mn}(t) = \int \frac{\mathrm{d}\omega}{2\pi} \rho^{(1)}_{mn}(\omega) \mathrm{e}^{-\mathrm{i}(\omega+\mathrm{i}\eta)t} \tag{E.8b}$$

results in

$$\rho^{(1)}_{mn}(\omega) = \frac{f_m - f_n}{\varepsilon_n - \varepsilon_m - \omega - \mathrm{i}\eta} \delta V_{\mathrm{eff},mn}(\omega), \tag{E.9}$$

where the $\eta > 0$ factor accounts for the adiabatically switching on of the perturbation in the past. Now, a new response function $R(\boldsymbol{r}, \boldsymbol{r}', t)$ can be introduced that relates the induced charge density linearly with the total effective perturbing potential (the factor of 2 accounts for the assumed spin degeneracy)

$$n_{\mathrm{ind}}(\boldsymbol{r}, \omega) = 2\rho^{(1)}(\boldsymbol{r}, \boldsymbol{r}, \omega) \equiv \int R(\boldsymbol{r}, \boldsymbol{r}', \omega) \delta V_{\mathrm{eff}}(\boldsymbol{r}', \omega) \, \mathrm{d}^3 r' \,. \tag{E.10}$$

This response function is directly found using (E.9),

$$\rho^{(1)}(\boldsymbol{r}, \boldsymbol{r}, \omega) = \sum_{m,n} \phi_m(\boldsymbol{r}) \rho^{(1)}_{mn}(\omega) \phi^*_n(\boldsymbol{r}) \tag{E.11}$$

and

$$\delta V_{\mathrm{eff},mn}(\omega) = \int \phi^*_m(\boldsymbol{r}) \delta V_{\mathrm{eff}}(\boldsymbol{r}, \omega) \phi_n(\boldsymbol{r}) \, \mathrm{d}^3 r \tag{E.12}$$

to be

$$R(\boldsymbol{r}, \boldsymbol{r}', \omega) = 2 \sum_{m,n} \frac{f_n - f_m}{\varepsilon_n - \varepsilon_m + \omega + \mathrm{i}\eta} \phi^*_n(\boldsymbol{r}) \phi_m(\boldsymbol{r}) \left(\phi^*_n(\boldsymbol{r}') \phi_m(\boldsymbol{r}') \right)^* . \tag{E.13}$$

In order to relate the response R to the dielectric function (1.12) we express it in terms of the response functions used in (1.16). For the susceptibility we find

$$\chi = \frac{\delta n^{\mathrm{ind}}}{\delta V^{\mathrm{ext}}} = \frac{\delta n^{\mathrm{ind}}}{\delta V^{\mathrm{eff}}} \left(1 + \frac{\delta V_{\mathrm{H}}}{\delta n^{\mathrm{ind}}} \frac{\delta n^{\mathrm{ind}}}{\delta V_{\mathrm{ext}}} + \frac{\delta V_{\mathrm{xc}}}{\delta n^{\mathrm{ind}}} \frac{\delta n^{\mathrm{ind}}}{\delta V_{\mathrm{ext}}} \right) = R + R(v + f_{\mathrm{xc}})\chi, \tag{E.14}$$

where

$$f_{\mathrm{xc}}(\boldsymbol{r}, t; \boldsymbol{r}', t') \coloneqq \frac{\delta V_{\mathrm{xc}}(\boldsymbol{r}, t)}{\delta n^{\mathrm{ind}}(\boldsymbol{r}', t')} \tag{E.15}$$

is the *exchange-correlation kernel*. A similar procedure relates R to the polarizability P according to

$$P = R + R f_{\mathrm{xc}} P. \tag{E.16}$$

Neglecting the exchange-correlation effects, i.e. setting $f_{\mathrm{xc}} = 0$ yields P and χ in the so called *Random-Phase-approximation* (RPA).

E.2. Dielectic matrix in RPA

In the RPA we neglect f_{xc} in eq. (E.16), so that $P^0 = R$ and write for the lattice Fourier transform of ε^0:

$$\varepsilon^0_{\boldsymbol{G}\boldsymbol{G}'}(\boldsymbol{q},\omega) = \delta_{\boldsymbol{G}\boldsymbol{G}'} - v_{\boldsymbol{G}}(\boldsymbol{q})P^0_{\boldsymbol{G}\boldsymbol{G}'}(\boldsymbol{q},\omega), \tag{E.17}$$

where the lattice Fourier transform of P^0 can be expressed using the plane wave matrix elements eq. (3.30) as

$$\begin{aligned} P^0_{\boldsymbol{G}\boldsymbol{G}'}(\boldsymbol{q},\omega) &= \frac{1}{V}\sum_{ou\boldsymbol{k}}\big(w_{ou\boldsymbol{k}}(\boldsymbol{q},\omega)M_{ou\boldsymbol{k}}(\boldsymbol{G},\boldsymbol{q})M^*_{ou\boldsymbol{k}}(\boldsymbol{G}',\boldsymbol{q}) \\ &\qquad + w_{uo\boldsymbol{k}}(\boldsymbol{q},\omega)M_{uo\boldsymbol{k}}(\boldsymbol{G},\boldsymbol{q})M^*_{uo\boldsymbol{k}}(\boldsymbol{G}',\boldsymbol{q})\big) \\ &=: P^{0,\mathrm{R}}_{\boldsymbol{G}\boldsymbol{G}'}(\boldsymbol{q},\omega) + P^{0,\mathrm{AR}}_{\boldsymbol{G}\boldsymbol{G}'}(\boldsymbol{q},\omega), \end{aligned} \tag{E.18}$$

where o (u) denotes occupied (unoccupied) states. The resonant and anti-resonant weights are defined as

$$w_{ou\boldsymbol{k}}(\boldsymbol{q},\omega) = \frac{f_{o\boldsymbol{k}} - f_{u\boldsymbol{k}+\boldsymbol{q}}}{\omega - \big(\varepsilon_{u\boldsymbol{k}+\boldsymbol{q}} - \varepsilon_{o\boldsymbol{k}}\big) + \mathrm{i}\delta} \quad w_{uo\boldsymbol{k}}(\boldsymbol{q},\omega) = \frac{f_{o\boldsymbol{k}+\boldsymbol{q}} - f_{u\boldsymbol{k}}}{-\omega - \big(\varepsilon_{u\boldsymbol{k}} - \varepsilon_{o\boldsymbol{k}+\boldsymbol{q}}\big) - \mathrm{i}\delta}. \tag{E.19}$$

The resonant and anti-resonant contributions are related by the symmetry properties of the plane-wave matrix elements as

$$P^{0,\mathrm{AR}}_{\boldsymbol{G}\boldsymbol{G}'}(\boldsymbol{q},\omega) = P^{0,\mathrm{R}*}_{-\boldsymbol{G}-\boldsymbol{G}'}(-\boldsymbol{q},-\omega). \tag{E.20}$$

Employing the time reversal symmetry yields another relation, namely

$$P^{0,\mathrm{AR}}_{\boldsymbol{G}\boldsymbol{G}'}(\boldsymbol{q},\omega) = P^{0,\mathrm{R}*}_{\boldsymbol{G}'\boldsymbol{G}}(\boldsymbol{q},-\omega). \tag{E.21}$$

Comparing eq. (E.13) and eq. (3.3) and neglecting the different time-ordering, one finds

$$\chi_0(\boldsymbol{r},\boldsymbol{r}',\boldsymbol{r},\boldsymbol{r}',\omega) = P^0(\boldsymbol{r},\boldsymbol{r}',-\omega) \tag{E.22}$$

if the quasi-particle wave-functions are replaced with the Kohn-Sham orbitals. The differing sign in the frequency stems from the choice to do the Fourier transform of the BSE eq. (2.24) in $t_2 - t_1$ instead of $t_1 - t_2$ in order to comply with [16].

We are interested in the case of static screening, i.e. $\omega = 0$, and we construct ε^0 without broadening, i.e. $\delta = 0$. In this case, it is

$$P^{0,\mathrm{AR}}_{\boldsymbol{G}\boldsymbol{G}'}(\boldsymbol{q},0) \overset{\mathrm{t.r.}}{=} P^{0,\mathrm{R}*}_{\boldsymbol{G}'\boldsymbol{G}}(\boldsymbol{q},0) \overset{\delta=0}{=} P^{0,\mathrm{R}}_{\boldsymbol{G}\boldsymbol{G}'}(\boldsymbol{q},0). \tag{E.23}$$

from which follows that eq. (E.18) reduces to

$$P^0_{\boldsymbol{G}\boldsymbol{G}'}(\boldsymbol{q},0) = 2P^{0,\mathrm{R}}_{\boldsymbol{G}\boldsymbol{G}'}(\boldsymbol{q},0). \tag{E.24}$$

F. Fourier Transform of L_0

In the construction of the matrix form of the Bethe-Salpeter equation the Fourier transform of the independent part L_0 of the two-particle correlation function L from the time to the frequency domain is needed. Since only electron-hole propagation is considered, L_0 only depends on one time difference $t = t_2 - t_1$, see section 2.3.4.

With the the definition of L_0 eq. (2.25) it is

$$L_0(\boldsymbol{r}_1, \boldsymbol{r}_2, \boldsymbol{r}_1', \boldsymbol{r}_2', t) = G_1(\boldsymbol{r}_1, \boldsymbol{r}_2', -t)G_1(\boldsymbol{r}_2, \boldsymbol{r}_1', t) \tag{F.1}$$

and using the independent quasiparticle approximation of G_1 eq. (2.20) we can write

$$\begin{aligned}L_0(\boldsymbol{r}_1, \boldsymbol{r}_2, \boldsymbol{r}_1', \boldsymbol{r}_2', \omega) &= \int \mathrm{d}t \iint \frac{\mathrm{d}\omega'}{2\pi}\frac{\mathrm{d}\omega''}{2\pi} G_1(\boldsymbol{r}_1, \boldsymbol{r}_2', \omega')G_1(\boldsymbol{r}_2, \boldsymbol{r}_1', \omega'')\mathrm{e}^{\mathrm{i}(\omega+\omega'-\omega'')t} \\ &= \int \frac{\mathrm{d}\omega'}{2\pi} G_1(\boldsymbol{r}_1, \boldsymbol{r}_2', \omega')G_1(\boldsymbol{r}_2, \boldsymbol{r}_1', \omega' + \omega) \\ &= \sum_{k,l} \int \frac{\mathrm{d}\omega'}{2\pi} \frac{\psi_k(\boldsymbol{r}_1)\psi_k^*(\boldsymbol{r}_2')\psi_l(\boldsymbol{r}_2)\psi_l^*(\boldsymbol{r}_1')}{\big(\omega' - \varepsilon_k + \mathrm{i}\delta\,\mathrm{sgn}(\varepsilon_k - E_\mathrm{f})\big)\big(\omega' + \omega - \varepsilon_l + \mathrm{i}\delta\,\mathrm{sgn}(\varepsilon_l - E_\mathrm{f})\big)}.\end{aligned} \tag{F.2}$$

Closing the contour in the upper half in the complex plane, the integral (F.2) is non-zero only if $\varepsilon_k > E_\mathrm{f} \wedge \varepsilon_l < E_\mathrm{f}$ or $\varepsilon_k < E_\mathrm{f} \wedge \varepsilon_l > E_\mathrm{f}$ and we get

$$\begin{aligned}L_0(\boldsymbol{r}_1, \boldsymbol{r}_2, \boldsymbol{r}_1', \boldsymbol{r}_2', \omega) = \mathrm{i} &\sum_{k,l} \psi_k(\boldsymbol{r}_1)\psi_k^*(\boldsymbol{r}_2')\psi_l(\boldsymbol{r}_2)\psi_l^*(\boldsymbol{r}_1') \\ &\times \left[-\frac{\Theta(\varepsilon_k - E_\mathrm{f})\Theta(E_\mathrm{f} - \varepsilon_l)}{\varepsilon_k - \varepsilon_l + \omega - \mathrm{i}\delta} + \frac{\Theta(E_\mathrm{f} - \varepsilon_k)\Theta(\varepsilon_l - E_\mathrm{f})}{\varepsilon_k - \varepsilon_l + \omega + \mathrm{i}\delta}\right].\end{aligned} \tag{F.3}$$

For an insulator without partial occupations we find in terms of the occupied (o) and unoccupied (u) states

$$\begin{aligned}L_0(\boldsymbol{r}_1, \boldsymbol{r}_2, \boldsymbol{r}_1', \boldsymbol{r}_2', \omega) &= -\mathrm{i} \sum_{o,u} \frac{\psi_u(\boldsymbol{r}_1)\psi_u^*(\boldsymbol{r}_2')\psi_o(\boldsymbol{r}_2)\psi_o^*(\boldsymbol{r}_1')}{\varepsilon_u - \varepsilon_o + \omega - \mathrm{i}\delta} + \frac{\psi_o(\boldsymbol{r}_1)\psi_o^*(\boldsymbol{r}_2')\psi_u(\boldsymbol{r}_2)\psi_u^*(\boldsymbol{r}_1')}{\varepsilon_u - \varepsilon_o - \omega - \mathrm{i}\delta} \\ &= -\mathrm{i} \sum_{o,u} \frac{\psi_o(\boldsymbol{r}_1)\psi_u^*(\boldsymbol{r}_1')\psi_o^*(\boldsymbol{r}_2')\psi_u(\boldsymbol{r}_2)}{\varepsilon_u - \varepsilon_o - \omega - \mathrm{i}\delta} + \frac{\psi_u(\boldsymbol{r}_1)\psi_o^*(\boldsymbol{r}_1')\psi_u^*(\boldsymbol{r}_2')\psi_o(\boldsymbol{r}_2)}{\varepsilon_u - \varepsilon_o + \omega - \mathrm{i}\delta} \\ &= \mathrm{i} \sum_{o,u} \frac{\psi_o(\boldsymbol{r}_1)\psi_u^*(\boldsymbol{r}_1')\psi_o^*(\boldsymbol{r}_2')\psi_u(\boldsymbol{r}_2)}{\omega - (\varepsilon_u - \varepsilon_o) + \mathrm{i}\delta} + \frac{\psi_u(\boldsymbol{r}_1)\psi_o^*(\boldsymbol{r}_1')\psi_u^*(\boldsymbol{r}_2')\psi_o(\boldsymbol{r}_2)}{-\omega - (\varepsilon_u - \varepsilon_o) + \mathrm{i}\delta}.\end{aligned} \tag{F.4}$$

Alternativley we can write eq. (F.3) for the insulator case equivalently as

$$
\begin{aligned}
L_0(\boldsymbol{r}_1, \boldsymbol{r}_2, \boldsymbol{r}_1', \boldsymbol{r}_2', \omega) &= -\mathrm{i} \sum_{k,l} \psi_k(\boldsymbol{r}_1)\psi_l^*(\boldsymbol{r}_1')\psi_k^*(\boldsymbol{r}_2')\psi_l(\boldsymbol{r}_2) \frac{\left|f_k - f_l\right|}{\left|\varepsilon_k - \varepsilon_l\right| + \omega\,\mathrm{sgn}(\varepsilon_k - \varepsilon_l) - \mathrm{i}\delta} \\
&= \mathrm{i} \sum_{k,l} \psi_k(\boldsymbol{r}_1)\psi_l^*(\boldsymbol{r}_1')\psi_k^*(\boldsymbol{r}_2')\psi_l(\boldsymbol{r}_2) \frac{\left|f_k - f_l\right|}{\omega\,\mathrm{sgn}(\varepsilon_l - \varepsilon_k) - \left|\varepsilon_k - \varepsilon_l\right| + \mathrm{i}\delta}
\end{aligned}
\tag{F.5}
$$

which can be used to treat partial occupancies in semiconductors. A factor of 2 can be introduced here to account for the spin degeneracy of the occupation factors.

Bibliography

1. Hambach, R. *Theory and ab-initio calculations of collective excitations in nanostructures: towards spatially-resolved EELS* Theses (Ecole Polytechnique X, Nov. 2010).
2. Hedin, L. & Lundqvist, S. in *Solid State Physics* (eds Seitz, F., Turnbull, D. & Ehrenreich, H.) (Elsevier Science, 1969). ISBN: 9780080864877.
3. Ambegaokar, V. & Kohn, W. Electromagnetic Properties of Insulators. I. *Physical Review* **117,** 423–431 (Jan. 1960).
4. Sole, R. D. & Fiorino, E. Macroscopic dielectric tensor at crystal surfaces. *Physical Review B* **29,** 4631–4645 (Apr. 1984).
5. Fetter, A. L. & Walecka, J. D. *Quantum Theory of Many-Particle Systems* 640 pp. ISBN: 0486428273 (Dover Publications Inc., 2003).
6. Adler, S. L. Quantum Theory of the Dielectric Constant in Real Solids. *Physical Review* **126,** 413–420 (Apr. 1962).
7. Wiser, N. Dielectric Constant with Local Field Effects Included. *Physical Review* **129,** 62–69 (Jan. 1963).
8. Onida, G., Reining, L. & Rubio, A. Electronic excitations: density-functional versus many-body Green's-function approaches. *Reviews of Modern Physics* **74,** 601–659 (June 2002).
9. Grosso, G. & Parravicini, G. P. *Solid State Physics* ISBN: 0-12-304460-X (Academic Press, 2000).
10. Pusching, P. *Excitonic Effects in Organic Semi-conductors* (2002).
11. Sagmeister, S. *Excitonic Effects in Solids* (2009).
12. Thomas, L. H. The calculation of atomic fields. *Mathematical Proceedings of the Cambridge Philosophical Society* **23,** 542 (Jan. 1927).
13. Fermi, E. Eine statistische Methode zur Bestimmung einiger Eigenschaften des Atoms und ihre Anwendung auf die Theorie des periodischen Systems der Elemente. *Zeitschrift für Physik* **48,** 73–79 (Jan. 1928).
14. Hohenberg, P. & Kohn, W. Inhomogeneous Electron Gas. *Physical Review* **136,** B864–B871 (Nov. 1964).
15. Kohn, W. & Sham, L. J. Self-Consistent Equations Including Exchange and Correlation Effects. 1. *Physical Review* **140,** A1133–A1138 (Nov. 1965).
16. Strinati, G. Application of the Green's functions method to the study of the optical properties of semiconductors. *La Rivista del Nuovo Cimento* **11,** 1–86 (Dec. 1988).

17. Roedl, C. *Elektronische und excitonische Anregungen in magnetischen Isolatoren* (2009).

18. Schwinger, J. The Theory of Quantized Fields. I. *Physical Review* **82,** 914–927 (June 1951).

19. Baym, G. & Kadanoff, L. P. Conservation Laws and Correlation Functions. *Physical Review* **124,** 287–299 (Oct. 1961).

20. Baym, G. Self-Consistent Approximations in Many-Body Systems. *Physical Review* **127,** 1391–1401 (Aug. 1962).

21. Hedin, L. New Method for Calculating the One-Particle Green's Function with Application to the Electron-Gas Problem. *Physical Review* **139,** A796–A823 (Aug. 1965).

22. Hybertsen, M. S. & Louie, S. G. First-Principles Theory of Quasiparticles: Calculation of Band Gaps in Semiconductors and Insulators. *Physical Review Letters* **55,** 1418–1421 (Sept. 1985).

23. Hybertsen, M. S. & Louie, S. G. Electron correlation in semiconductors and insulators: Band gaps and quasiparticle energies. *Physical Review B* **34,** 5390–5413 (Oct. 1986).

24. Strinati, G. Dynamical Shift and Broadening of Core Excitons in Semiconductors. *Physical Review Letters* **49,** 1519–1522 (Nov. 1982).

25. Mattuck, R. D. *A Guide to Feynman Diagrams in the Many-Body Problem* 429 pp. ISBN: 0486670473 (Dover Publications Inc., Nov. 1, 1992).

26. Sander, T., Maggio, E. & Kresse, G. Beyond the Tamm-Dancoff approximation for extended systems using exact diagonalization. *Physical Review B* **92.** doi:`10.1103/physrevb.92.045209` (July 2015).

27. Furche, F. On the density matrix based approach to time-dependent density functional response theory. *The Journal of Chemical Physics* **114,** 5982–5992 (Apr. 2001).

28. Rosenfeld, L. *Theory of Electrons* 68 ff (New York: Dover Publications, 1965).

29. Neil W. Ashcroft, N. M. *Solid State Physics* 848 pp. ISBN: 0030839939 (Cengage Learning, Inc, 1976).

30. Schwabl, F. *Quantenmechanik für Fortgeschrittene (QM II)* 432 pp. ISBN: 3540850759 (Springer, 2008).

31. Koelling, D. D. & Harmon, B. N. A technique for relativistic spin-polarised calculations. *Journal of Physics C: Solid State Physics* **10,** 3107–3114 (Aug. 1977).

32. Ehrenreich, H. & Cohen, M. H. Self-Consistent Field Approach to the Many-Electron Problem. *Physical Review* **115,** 786–790 (Aug. 1959).